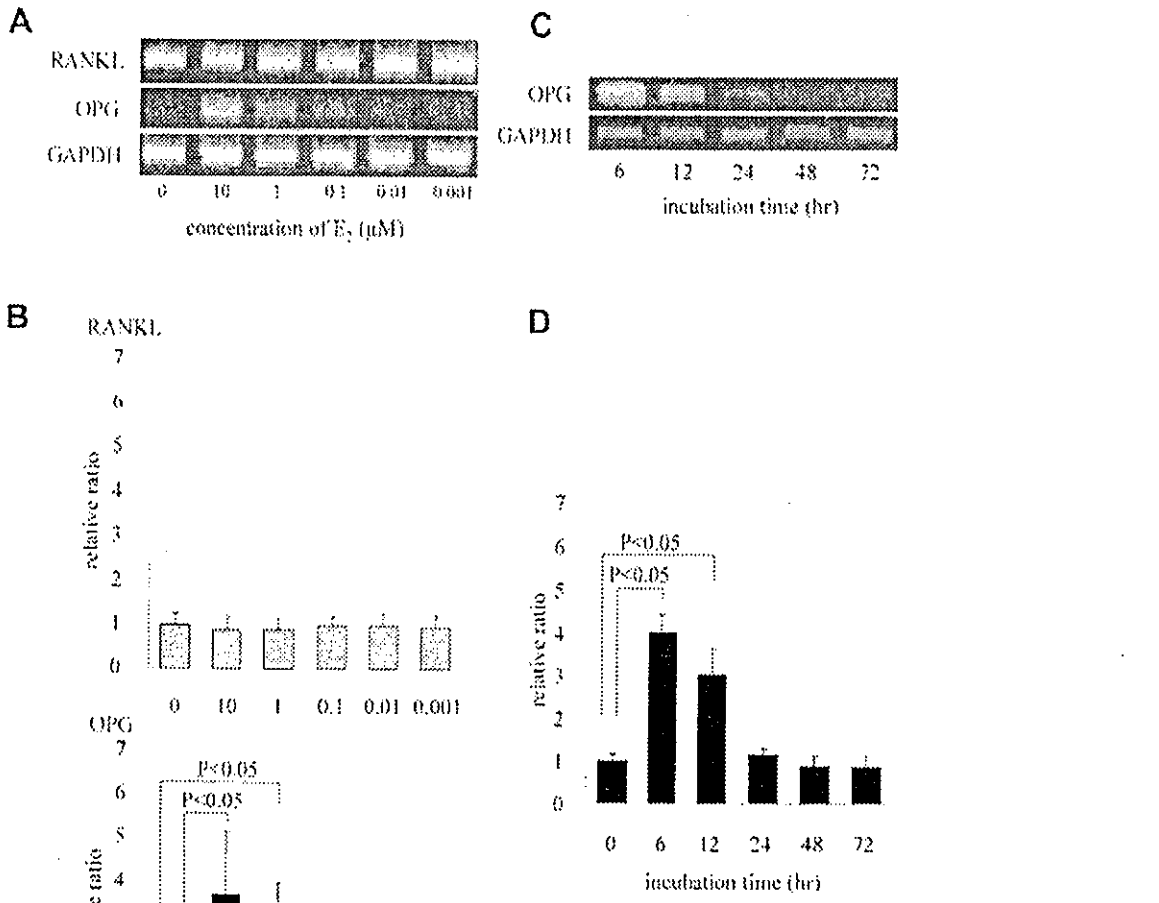

Figure 2. Expression of RANKL and OPG mRNA in RA-FLS treated with E2. (A), Dose dependency: RA-FLS were incubated with various concentrations of E2 (10^{-5}-10^{-9} M) for 12 h or untreated. (B), Fold increases of RANKL (upper panel) and OPG (lower panel) mRNA by E2 treatment. E2 enhanced OPG mRNA expression at the concentrations of 10^{-6} and 10^{-5} M ($P<0.05$), but did not increase RANKL mRNA. (C), Time-course study: RA-FLS were treated with 10^{-6} M E2 for the incubation period indicated. (D), Fold increases of RANKL and OPG mRNA of time-course study. The effect of E2 reached the peak at 6 h, declined thereafter for 12 h and was almost abolished after 24 h ($P<0.05$).

and CATGTGGGCCATGAGGTCCACCAC. After PCR amplification, 8 μl aliquots of the PCR products were electrophoresed in 2.0% agarose gels and stained with ethidium bromide. PCR products were photographed and quantified using the public domain NIH Image program (developed at the US National Institutes of Health and available on the Internet at http://rsb.info.nih.gov/nih-image/). Values were normalized to GAPDH expression.

Enzyme-linked immunosorbent assay OPG assay. RA-FLS were cultured in a 24-well plate at a cell density of $1.0x10^5$/well in DMEM supplemented with 10% FBS. When the cultured RA-FLS reached confluence, they were incubated with E2 or tamoxifen. After 6, 12, 24, and 48 h of incubation, the concentration of OPG in the culture supernatants was measured with using OPG enzyme-linked immunosorbent assay system (Immundiagnostik, Bensheim, Germany) according to the manufacturer's instructions. The OPG concentration was determined from the mean value of triplicate samples. Statistical analyses were performed by One-way ANOVA and Fisher's PLSD. A $P<0.05$ were considered to be statistically significant.

Results

Expression of ER-α and ER-β mRNA in RA-FLS. To determine the presence of ER-α and ER-ß in FLS, we utilized RT-PCR to amplify ER mRNA from FLS of patients with RA and osteoarthritis (OA) (Fig. 1A). The results indicated that mRNA of ER-α and ER-ß was specifically amplified in all 6 RA and 5 OA samples, the specificity of which was confirmed by DNA sequencing (data not shown). The effect of E2 on the expression of ER-α and ER-ß was examined in RA-FLS using RT-PCR; E2 significantly enhanced ER-α mRNA expression in RA-FLS in a dose-dependent manner ($P<0.05$), whereas ER-ß mRNA expression was unaffected (Fig. 1B and C). Co-treatment with a specific estrogen antagonist, ICI 182780, completely abrogated the stimulatory effects of E2 (10^{-6} M) on ER-α in RA-FLS (Fig. 1D and E).

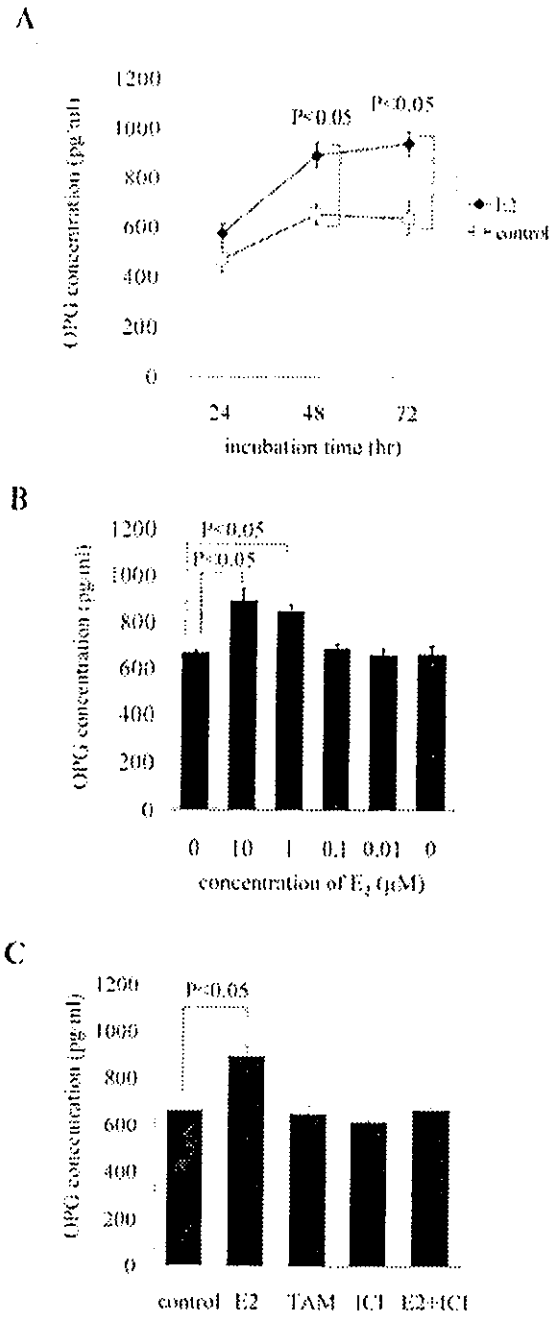

Figure 3. E2-induced OPG protein secretion from RA-FLS. (A), Time dependency: RA-FLS were treated with 10^{-6} M E2 for the incubation period indicated. The values are given as the mean ± SEM of triplicates (P<0.05). OPG secreted by RA-FLS treated with 10^{-6} M E2 was significantly higher than untreated RA-FLS at 48 and 72 h (P<0.05). (B), Dose dependency: RA-FLS were treated with various concentrations of E2 (10^{-5}-10^{-9} M) for 12 h or untreated. Treatment with E2 at the concentrations of 10^{-6} and 10^{-5} M increased OPG secretion from RA-FLS at 48 h (P<0.05). (C), Treatment with tamoxifen (TAM) and ICI 182780 (ICI). Co-treatment with 10^{-5} M ICI 182780 completely abrogated the stimulatory effects of E2 (10^{-6} M) on OPG secretion. Tamoxifen (10^{-6} M) did not increase OPG secretion from RA-FLS.

mRNA expression of OPG and RANKL in RA-FLS. RT-PCR indicated that E2 enhanced OPG mRNA expression at concentrations greater than 10^{-6} M (P<0.05), whereas RANKL mRNA expression was unaffected (Fig. 2A and B). A time-course study revealed that 10^{-6} M of E2 enhanced OPG mRNA expression as early as 6 h after treatment, and that the effect of E2 peaked at 6 h and declined thereafter, up to 12 h (P<0.05; Fig. 2C and D). The effect of E2 was almost abolished after 24 h.

Effect on OPG secretion in RA-FLS. The amount of OPG secreted from RA-FLS to culture supernatants was significantly increased after treatment with 10^{-6} M E2, as compared with untreated controls at 48 and 72 h (P<0.05) (Fig. 3A). E2 at concentrations greater than 10^{-6} M increased OPG secretion after 48 h (P<0.05; Fig. 3B). While co-treatment with 10^{-5} M ICI 182780 completely abrogated the stimulatory effects of E2 (10^{-6} M) on OPG secretion, tamoxifen (10^{-6} M) did not increase OPG secretion from RA-FLS (Fig. 3C).

Discussion

Until recently, inflammatory cytokines, such as interleukin (IL)-1, IL-6, IL-11, and TNF-α, were implicated as important mediators of bone lysis (26-28). Recent findings, however, indicate that osteoclasts have a substantial role in bone destruction, and that RANKL might be the central mediator of osteoclast development in RA and other bone loss pathologies. Osteoclasts are observed at the invasive front of granulomatous synovial tissues in both RA and animal models of arthritis (5,29). RANKL expressed on synovial fibroblasts and activated T lymphocytes enhances differentiation of synovial macrophages and osteoclast precursors in bone marrow into bone-resorbing osteoclasts, and activates osteoclasts at sites of bone erosion in RA (6,30,31). Further, Kong *et al* reported that joint destruction, but not synovial inflammation, was significantly improved by OPG treatment in rodent models of adjuvant arthritis (32). While RANK, RANKL, and OPG are all expressed in rheumatoid synovial tissues, their relative balance is important for determining the extent of osteoclastic bone resorption and is considered to be a good therapeutic target (6,7,28).

We demonstrate that 17ß-estradiol enhances the expression of ER-α in RA-FLS without affecting the expression of ER-ß and that E2 stimulates the production of OPG from RA-FLS without affecting RANKL expression. We therefore hypothesize that estrogen prevents bone erosion by up-regulating OPG production from RA-FLS via ER-α to increase OPG binding of RANKL, which subsequently blocks the interaction between RANKL and RANK in osteoclasts.

Despite the number of studies performed to date, the effect of sex hormones on RA remains controversial. *In vitro* studies indicate that estrogen regulates proteinases and inflammatory cytokines, such as matrix metalloproteinase (MMP) and IL-1ß-induced IL-6, and thus estrogen potentiates the destruction of cartilage and bone in RA (12,13). Positive and negative results have been reported with regard to hormone replacement therapy (HRT) with estrogens (33-37). Nevertheless, type-II collagen-induced arthritis in female mice is exacerbated by ovariectomy and is ameliorated by subsequent treatment with E2 (38). Furthermore, a recent trial exploring the effects in RA demonstrated that HRT significantly ameliorated inflammation, disease activity, and osteoporosis of RA, and retarded the progression of joint destruction (39).

In the present study we demonstrated that 17ß-estradiol increases ER-α mRNA and OPG mRNA expression, and the OPG protein released in the culture supernatant was simultaneously increased in each line of RA-FLS. Importantly, the increase of OPG and ER-α was specifically antagonized by ICI 182780, an estrogen specific antagonist. Further, in RA-FLS, OPG, but not RANKL, was increased by 17ß-estradiol.

Interestingly, a selective ER modulator (SERM), tamoxifen, which acts as a weak estrogen agonist on bone *in vivo*, did not affect OPG production of RA-FLS. As tamoxifen is reported to abrogate the effect of E2 to increase MMP in RA-FLS (12), tamoxifen might function as an antagonist rather than as an agonist of E2 in RA-FLS. Raloxifene, a SERM member, however, stimulates OPG and inhibits IL-6 production in human trabecular osteoblasts (40). Further studies regarding the modulation of OPG production of RA-FLS, SERMs, and the other modulators will be important to prevent bone erosion on RA.

References

1. Shimizu S, Shiozawa S, Shiozawa K, Imura S and Fujita T: Quantitative histologic studies on the pathogenesis of periarticular osteoporosis in rheumatoid arthritis. Arthritis Rheum 28: 25-31, 1985.
2. Van Zeben D, Hazes JM, Breedveld FC, Zwinderman AH and Vandenbroucke JP: Which clinical variables contribute to the physician's assessment of medium term outcome in rheumatoid arthritis? J Rheumatol 20: 33-39, 1993.
3. Fujikawa Y, Shingu M, Torisu T, Itonaga I and Masumi S: Bone resorption by tartrate-resistant acid phosphatase-positive multinuclear cells isolated from rheumatoid synovium. Br J Rheumatol 35: 213-217, 1996.
4. Takayanagi H, Oda H, Yamamoto S, Kawaguchi H, Tanaka S, Nishikawa T and Koshihara Y: A new mechanism of bone destruction in rheumatoid arthritis: synovial fibroblasts induce osteoclastogenesis. Biochem Biophys Res Commun 240: 279-286, 1997.
5. Gravallese EM, Harada Y, Wang JT, Gorn AH, Thornhill TS and Goldring SR: Identification of cell types responsible for bone resorption in rheumatoid arthritis and juvenile rheumatoid arthritis. Am J Pathol 152: 943-951, 1998.
6. Takayanagi H, Iizuka H, Juji T, Nakagawa T, Yamamoto A, Miyazaki T, Koshihara Y, Oda H, Nakamura K and Tanaka S: Involvement of receptor activator of nuclear factor kappaB ligand/osteoclast differentiation factor in osteoclastogenesis from synoviocytes in rheumatoid arthritis. Arthritis Rheum 43: 259-269, 2000.
7. Haynes DR, Crotti TN, Loric M, Bain GI, Atkins GJ and Findlay DM: Osteoprotegerin and receptor activator of nuclear factor kappaB ligand (RANKL) regulate osteoclast formation by cells in the human rheumatoid arthritic joint. Rheumatology 40: 623-630, 2001.
8. Yasuda H, Shima N, Nakagawa N, Yamaguchi K, Kinosaki M, Mochizuki S, Tomoyasu A, Yano K, Goto M, Murakami A, Tsuda E, Morinaga T, Higashio K, Udagawa N, Takahashi N and Suda T: Osteoclast differentiation factor is a ligand for osteoprotegerin/osteoclastogenesis-inhibitory factor and is identical to TRANCE/RANKL. Proc Natl Acad Sci USA 95: 3597-3602, 1998.
9. Lacey DL, Timms E, Tan HL, Kelley MJ, Dunstan CR, Burgess T, Elliott R, Colombero A, Elliott G, Scully S, Hsu H, Sullivan J, Hawkins N, Davy E, Capparelli C, Eli A, Qian YX, Kaufman S, Sarosi I, Shalhoub V, Senaldi G, Guo J, Delaney J and Boyle WJ: Osteoprotegerin ligand is a cytokine that regulates osteoclast differentiation and activation. Cell 93: 165-176, 1998.
10. Simonet WS, Lacey DL, Dunstan CR, Kelley M, Chang MS, Luthy R, Nguyen HQ, Wooden S, Bennett L, Boone T, Shimamoto G, De Rose M, Elliott R, Colombero A, Tan HL, Trail G, Sullivan J, Davy E, Bucay N, Renshaw-Gegg L, Hughes TM, Hill D, Pattison W, Campbell P, Boyle WJ, *et al*: Osteoprotegerin: a novel secreted protein involved in the regulation of bone density. Cell 89: 309-319, 1997.
11. Yasuda H, Shima N, Nakagawa N, Mochizuki SI, Yano K, Fujise N, Sato Y, Goto M, Yamaguchi K, Kuriyama M, Kanno T, Murakami A, Tsuda E, Morinaga T and Higashio K: Identity of osteoclastogenesis inhibitory factor (OCIF) and osteo-protegerin (OPG): a mechanism by which OPG/OCIF inhibits osteoclastogenesis *in vitro*. Endocrinology 139: 1329-1337, 1998.
12. Khalkhali-Ellis Z, Seftor EA, Nieva DR, Handa RJ, Price RH, Jr, Kirschmann DA, Baragi VM, Sharma RV, Bhalla RC, Moore TL and Hendrix MJ: Estrogen and progesterone regulation of human fibroblast-like synoviocyte function *in vitro*: implications in rheumatoid arthritis. J Rheumatol 27: 1622-1631, 2000.
13. Kawasaki T, Ushiyama T, Inoue K and Hukuda S: Effects of estrogen on interleukin-6 production in rheumatoid fibroblast-like synoviocytes. Clin Exp Rheumatol 18: 743-745, 2000.
14. Masi AT: Hormonal and immunologic risk factors for the development of rheumatoid arthritis: an integrative physiopathogenetic perspective. Rheum Dis Clin North Am 26: 775-803, 2000.
15. Masi AT: Incidence of rheumatoid arthritis: do the observed age-sex interaction patterns support a role of androgenic-anabolic steroid deficiency in its pathogenesis? Br J Rheumatol 33: 697-699, 1994.
16. Rudge SR, Kowanko IC and Drury PL: Menstrual cyclicity of finger joint size and grip strength in patients with rheumatoid arthritis. Ann Rheum Dis 42: 425-430, 1983.
17. Persellin RH: The effect of pregnancy on rheumatoid arthritis. Bull Rheum Dis 27: 922-927, 1976.
18. Katzenellenbogen BS: Estrogen receptors: bioactivities and interactions with cell signaling pathways. Biol Reprod 54: 287-293, 1996.
19. Kuiper GG, Enmark E, Pelto-Huikko M, Nilsson S and Gustafsson JA: Cloning of a novel receptor expressed in rat prostate and ovary. Proc Natl Acad Sci USA 93: 5925-5930, 1996.
20. Greene GL, Gilna P, Waterfield M, Baker A, Hort Y and Shine J: Sequence and expression of human estrogen receptor complementary DNA. Science 231: 1150-1154, 1986.
21. Tora L, White J, Brou C, Tasset D, Webster N, Scheer E and Chambon P: The human estrogen receptor has two independent nonacidic transcriptional activation functions. Cell 59: 477-487, 1989.
22. Ishizuka M, Hatori M, Suzuki T, Miki Y, Darnel AD, Tazawa C, Sawai T, Uzuki M, Tanaka Y, Kokubun S and Sasano H: Sex steroid receptors in rheumatoid arthritis. Clin Sci 00: 000-000, 2003.
23. Bord S, Ireland DC, Beavan SR and Compston JE: The effects of estrogen on osteoprotegerin, RANKL, and estrogen receptor expression in human osteoblasts. Bone 32: 136-141, 2003.
24. Hofbauer LC, Khosla S, Dunstan CR, Lacey DL, Spelsberg TC and Riggs BL: Estrogen stimulates gene expression and protein production of osteoprotegerin in human osteoblastic cells. Endocrinology 140: 4367-4370, 1999.
25. Arnett FC, Edworthy SM, Bloch DA, McShane DJ, Fries JF, Cooper NS, Healey LA, Kaplan SR, Liang MH, Luthra HS, *et al*: The American Rheumatism Association 1987 revised criteria for the classification of rheumatoid arthritis. Arthritis Rheum 31: 315-324, 1988.
26. Chu CQ, Field M, Allard S, Abney E, Feldmann M and Maini RN: Detection of cytokines at the cartilage/pannus junction in patients with rheumatoid arthritis: implications for the role of cytokines in cartilage destruction and repair. Br J Rheumatol 31: 653-661, 1992.
27. Deleuran BW, Chu CQ, Field M, Brennan FM, Katsikis P, Feldmann M and Maini RN: Localization of interleukin-1 alpha, type 1 interleukin-1 receptor and interleukin-1 receptor antagonist in the synovial membrane and cartilage/pannus junction in rheumatoid arthritis. Br J Rheumatol 31: 801-809, 1992.
28. Kotake S, Udagawa N, Hakoda M, Mogi M, Yano K, Tsuda E, Takahashi K, Furuya T, Ishiyama S, Kim KJ, Saito S, Nishikawa T, Takahashi N, Togari A, Tomatsu T, Suda T and Kamatani N: Activated human T cells directly induce osteoclastogenesis from human monocytes: possible role of T cells in bone destruction in rheumatoid arthritis patients. Arthritis Rheum 44: 1003-1012, 2001.
29. Suzuki Y, Nishikaku F, Nakatuka M and Koga Y: Osteoclast-like cells in murine collagen induced arthritis. J Rheumatol 25: 1154-1160, 1998.
30. Gravallese EM, Manning C, Tsay A, Naito A, Pan C, Amento E and Goldring SR: Synovial tissue in rheumatoid arthritis is a source of osteoclast differentiation factor. Arthritis Rheum 43: 250-258, 2000.

31. Schett G, Redlich K and Smolen JS: The role of osteoprotegerin in arthritis. Arthritis Res Ther 5: 239-245, 2003.
32. Kong YY, Feige U, Sarosi I, Bolon B, Tafuri A, Morony S, Capparelli C, Li J, Elliott R, McCabe S, Wong T, Campagnuolo G, Moran E, Bogoch ER, Van G, Nguyen LT, Ohashi PS, Lacey DL, Fish E, Boyle WJ and Penninger JM: Activated T cells regulate bone loss and joint destruction-in adjuvant arthritis through osteoprotegerin ligand. Nature 402: 304-309, 1999.
33. D'Elia HF, Mattsson LA, Ohlsson C, Nordborg E and Carlsten H: Hormone replacement therapy in rheumatoid arthritis is associated with lower serum levels of soluble IL-6 receptor and higher insulin-like growth factor 1. Arthritis Res Ther 5: R202-R209, 2003.
34. Brennan P, Bankhead C, Silman A and Symmons D: Oral contraceptives and rheumatoid arthritis: results from a primary care-based incident case-control study. Semin Arthritis Rheum 26: 817-823, 1997.
35. Ostensen M: Sex hormones and pregnancy in rheumatoid arthritis and systemic lupus erythematosus. Ann NY Acad Sci 876: 131-144, 1999.
36. Hall GM, Daniels M, Huskisson EC and Spector TD: A randomised controlled trial of the effect of hormone replacement therapy on disease activity in postmenopausal rheumatoid arthritis. Ann Rheum Dis 53: 112-116, 1994.
37. Van den Brink HR, van Everdingen AA, van Wijk MJ, Jacobs JW and Bijlsma JW: Adjuvant oestrogen therapy does not improve disease activity in postmenopausal patients with rheumatoid arthritis. Ann Rheum Dis 52: 862-865, 1993.
38. Holmdahl R, Jansson L, Meyerson B and Klareskog L: Oestrogen induced suppression of collagen arthritis: I. Long term oestradiol treatment of DBA/1 mice reduces severity and incidence of arthritis and decreases the anti type II collagen immune response. Clin Exp Immunol 70: 372-378, 1987.
39. D'Elia HF, Larsen A, Mattsson LA, Waltbrand E, Kvist G, Mellstrom D, Saxne T, Ohlsson C, Nordborg E and Carlsten H: Influence of hormone replacement therapy on disease progression and bone mineral density in rheumatoid arthritis. J Rheumatol 30: 1456-1463, 2003.
40. Viereck V, Grundker C, Blaschke S, Niederkleine B, Siggelkow H, Frosch KH, Raddatz D, Emons G and Hofbauer LC: Raloxifene concurrently stimulates osteoprotegerin and inhibits interleukin-6 production by human trabecular osteoblasts. J Clin Endocrinol Metab 88: 4206-4213, 2003.

Design, Synthesis, and Biological Evaluation of New Cyclic Disulfide Decapeptides That Inhibit the Binding of AP-1 to DNA

Keiichi Tsuchida,*,† Hisaaki Chaki,‡ Tadakazu Takakura,† Junichi Yokotani,† Yukihiko Aikawa,‡ Shunichi Shiozawa,§,∥ Hiroaki Gouda,⊥ and Shuichi Hirono⊥

Discovery Laboratories and Research Laboratories, Toyama Chemical Co., Ltd., 4-1 Shimookui 2-chome, Toyama 930-8508, Japan, Department of Rheumatology, Faculty of Health Science, Kobe University School of Medicine, 7-10-2 Tomogaoka, Suma-ku, Kobe 654-0142, Japan, Rheumatic Disease Division, Kobe University Hospital, 7-5-2 Kusunoki-cho, Chuo-ku, Kobe 650-0017, Japan, and School of Pharmaceutical Sciences, Kitasato University, 5-9-1 Shirokane, Minato-ku, Tokyo 108-8641, Japan

Received February 4, 2004

The transcription factor activator protein-1 (AP-1) is an attractive target for the treatment of immunoinflammatory diseases, such as rheumatoid arthritis. Using the three-dimensional (3D) X-ray crystallographic structure of the DNA-bound basic region leucine zipper (bZIP) domains of AP-1, new cyclic disulfide decapeptides were designed and synthesized that demonstrated AP-1 inhibitory activities. The most potent inhibition was exhibited by Ac-c[Cys-Gly-Gln-Leu-Asp-Leu-Ala-Asp-Gly-Cys]-NH_2 (peptide **2**) (IC_{50} = 8 μM), which was largely due to the side chains of residues 3–6 and 8 of the peptide, as shown by an alanine scan. To provide structural information about the biologically active conformation of peptide **2**, the structures of peptide **2** derived from molecular dynamics simulation of the bZIP–peptide **2** complex with explicit water molecules were superimposed on the solution structures derived from NMR measurements of peptide **2** in water. These showed a strong structural similarity in the backbones of residues 3–7 and enabled the construction of a 3D pharmacophore model of AP-1 binding compounds, based on the chemical and structural features of the amino acid side chains of residues 3–7 in peptide **2**.

Introduction

Activator protein-1 (AP-1) is an important transcription factor for genes involved in immune and inflammatory responses, such as cytokines and collagenase.[1-3] Various inflammatory and mitogenic stimulations lead to AP-1 activation, and it probably plays a role in rheumatoid arthritis, transplant rejection, and tumor growth, so it is an attractive therapeutic target for the treatment of such disorders.[4] Indeed, systematic administration of an AP-1 decoy oligodeoxynucleotide containing the AP-1 binding site was found to inhibit arthritic joint destruction in mice with collagen-induced arthritis.[5] AP-1 is composed of members of the Fos and Jun families.[1] Fos and Jun proteins dimerize through a leucine zipper motif at their carboxyl terminals and bind DNA through a basic region that is located immediately upstream of the leucine zipper.[1,6] The three-dimensional (3D) X-ray crystallographic structure[7] of the basic region leucine zipper (bZIP) domains of c-Fos and c-Jun bound to a 20 nucleotide DNA duplex containing the AP-1 binding site revealed single α-helices and showed that the heterodimer grips the major groove of the DNA like a pair of forceps. Although the solution structure of the bZIP domains of AP-1 in the absence of DNA is unclear, the effect of dimerization and DNA binding on circular dichroism (CD) spectra of the bZIP domains suggested that the basic regions of the domains take on an α-helical conformation only in the presence of DNA.[8] In support of this, the solution structure of the yeast transcriptional factor GCN4 bZIP domain, as determined by NMR, revealed that the leucine zipper region forms a long uninterrupted α-helix and the basic region is flexible but structured, fluctuating around a helical conformation in the absence of DNA.[9]

Structure-based drug design methods have strongly enhanced the lead discovery and optimization process using the 3D structures of target proteins, which are important for understanding the interaction between the ligand and the target protein.[10,11] Recently, natural products such as curcumin,[12,13] dihydroguaiaretic acid,[12,14] momordin,[15] and a new anthraquinone derivative[16] were reported to inhibit the binding of AP-1 to the AP-1 binding site. However, 3D structural information about the AP-1 binding of these inhibitors is not yet available.

We therefore carried out the de novo design of cyclic peptides exhibiting AP-1 inhibitory activity using the 3D structure of the bZIP domains from the X-ray crystal structure of the AP-1–DNA complex.[7] Our aim was to construct a hypothetical 3D pharmacophore model for generating new AP-1 inhibitors. A pharmacophore model is defined as the 3D arrangement of the structural and physicochemical features that are relevant to biological activity and is a versatile tool to aid in the discovery and development of new lead compounds.[17]

Cyclization of a flexible linear peptide is known to reduce the conformational freedom of the peptide and restrict its possible conformations, often resulting in

* To whom correspondence should be addressed. Tel: +81-76-431-8218. Fax: +81-76-431-8208. E-mail: KEIICHI_TUCHIDA@toyama-chemical.co.jp.
† Discovery Laboratories, Toyama Chemical Co., Ltd.
‡ Research Laboratories, Toyama Chemical Co., Ltd.
§ Kobe University School of Medicine.
∥ Kobe University Hospital.
⊥ Kitasato University.

10.1021/jm049890+ CCC: $27.50
Published on Web 07/21/2004

higher receptor binding affinity.[18,19] Several methods for cyclization are known, and we selected the disulfide method, which forms a side chain−side chain disulfide bridge between the N- and the C-terminal Cys residues.

Here, we report the rational design and synthesis of cyclic disulfide decapeptides and their inhibitory activities as evaluated by an AP-1 binding assay. Ac-*c*[Cys-Gly-Gln-Leu-Asp-Leu-Ala-Asp-Gly-Cys]-NH_2 (peptide **2**) exhibited the most potent inhibitory activity (IC_{50} = 8 μM) among these peptides. Furthermore, we built a pharmacophore model based on the chemical and structural features of peptide **2** obtained from an alanine scan and structural studies using a combination of NMR and molecular dynamics (MD) simulations of peptide **2**.

Methods

Molecular Modeling and de Novo Design. The crystallographic coordinates of the bZIP domains of AP-1 were obtained from the Brookhaven Protein Data Bank, entry 1FOS,[7] followed by the addition of hydrogen atoms to the bZIP domains with standard geometry. All molecular modeling and docking studies were performed using the SYBYL software package version 6.4[20] running on a Silicon Graphics Power Indigo2 workstation. All of the peptides used in this study were built using the Biopolymer module. The designed peptides were N-terminal-acetylated and C-terminal-amidated. Ionizable residues in the bZIP domains and designed peptides were assumed to be charged under physiological conditions. Docking was performed with the manual docking module DOCK. Our design was based on the AP-1 DNA binding site topology from the X-ray crystal structure of the AP-1−DNA complex. In the complex, Asn147 and Arg155 of c-Fos and Asn271 of c-Jun interact with the bases of the AP-1 binding site by hydrogen bonds, whereas the β-carbons of Ala150, Ala151 and Ser154 of c-Fos and Ala274, Ala275 and Ser278 of c-Jun come in contact with the 5-methyl groups of thymine bases of the AP-1 binding site by hydrophobic interactions.[7] The residues involved in these interactions are essential for the high-affinity binding of AP-1 to DNA.[21−26] On the basis of these interactions between the bZIP domains and the DNA, the candidate peptides were manually docked in the binding site. In particular, several spatial orientations and conformations of peptides were evaluated in the binding site of the bZIP domains.

Minimization of each complex obtained by docking was performed to reach a final convergence of 0.001 kcal mol^{-1} $Å^{-1}$ by the Powell method in the MAXIMIN2 module of SYBYL. The Tripos force field[27] was used for the energy minimizations, and a dielectric constant of 78.3 was employed. Partial atomic charges were calculated by the method of Gasteiger and Hückel.[28,29] The intermolecular energy of the peptide−binding site interaction was used to evaluate the quality of the docking experiment.

MD Simulations. The MD calculations were performed with AMBER version 4.1.[30] The structure of the bZIP−peptide **1** (Ac-*c*[Cys-Gly-Gln-Leu-Asp-Leu-Ala-Leu-Gly-Cys]-NH_2) complex obtained by docking was covered with an 18 Å shell of 9163 water molecules. The TIP3P model was used as the water model.[31] The resulting structure of the complex was optimized using energy minimization until the root-mean-square (RMS) value of the potential gradient was <0.05 kcal mol^{-1} $Å^{-1}$. MD simulation was then performed for 100 ps at 310 K with a dielectric constant of 1.0. Next, the initial structure of the bZIP−peptide **2** complex was constructed by the replacement of Leu in position 8 of peptide **1** with Asp while maintaining the original side chain orientation in the bZIP−peptide **1** complex after removing water molecules using the Biopolymer module of SYBYL 6.4. The structure obtained was covered with a 22 Å shell of 12 810 water molecules. After energy minimization of the structure, MD simulation was carried out for a period of 400 ps. The model structure obtained after MD simulation was minimized using the conditions described above.

The SHAKE algorithm was employed to restrain the bond lengths in order to remove the high-frequency motions.[32] This allowed us to use a time step of 1 fs. We used the dual nonbonded cutoff method with a primary cutoff of 9 Å and a secondary cutoff of 12 Å. The nonbonded pair list was updated every 20 time steps in the MD calculations. All calculations were carried out using a Silicon Graphics Power Indigo2 workstation.

Results and Discussion

De Novo Design. We designed candidate peptides using a combination of aliphatic hydrophobic amino acids such as Leu, Ile, and Val, acidic amino acids such as Asp and Glu, and neutral polar amino acids such as Asn and Gln. bZIP domains lack a binding cavity, so we chose a manual rather than an automated docking procedure. First, we searched for a tripeptide to interact with the residues, Asn147, Ala150, Ala151, Ser154, and Arg155 in the basic region of c-Fos, which participate in contacts with the bases of the AP-1 binding site of DNA. We chose Ac-Asn-Leu-Asp-NH_2 to assume the hydrogen-bonding interaction between the Asn residue and the Asn147 and between the Asp residue and the Arg155 and the hydrophobic interaction between the Leu residue and the residues, Ala150, Ala151, and Ser154, and then, we docked the tripeptide into the binding site of the bZIP domains (Figure 1a). Next, we elongated the tripeptide stepwise at the C terminus by one residue increments to the hexapeptide Ac-Asn-Leu-Asp-Leu-Ala-Leu-NH_2 to interact with the residues Asn271, Ala274, Ala275, and Ser278 in the basic region of c-Jun. Finally, we built the cyclic disulfide decapeptide Ac-*c*[Cys-Gly-Asn-Leu-Asp-Leu-Ala-Leu-Gly-Cys]-NH_2 by addition of Cys-Gly residues at the N terminus and Gly-Cys residues at the C terminus to the hexapeptide and by cyclization of the resulting decapeptide. On the basis of the docking model of the cyclic peptide, we designed several cyclic peptides by replacement of a residue of the cyclic peptide by appropriate residue to assume an interaction with the putative binding site in the bZIP domains. By way of example, Figure 1b shows the docking model of peptide **1**, obtained by replacement of Asn3 with Gln and energy minimization. After evaluating the quality of the docking experiment by the interaction energy between the designed peptide and the bZIP domains, decapeptides with relatively large interaction energies were synthe-

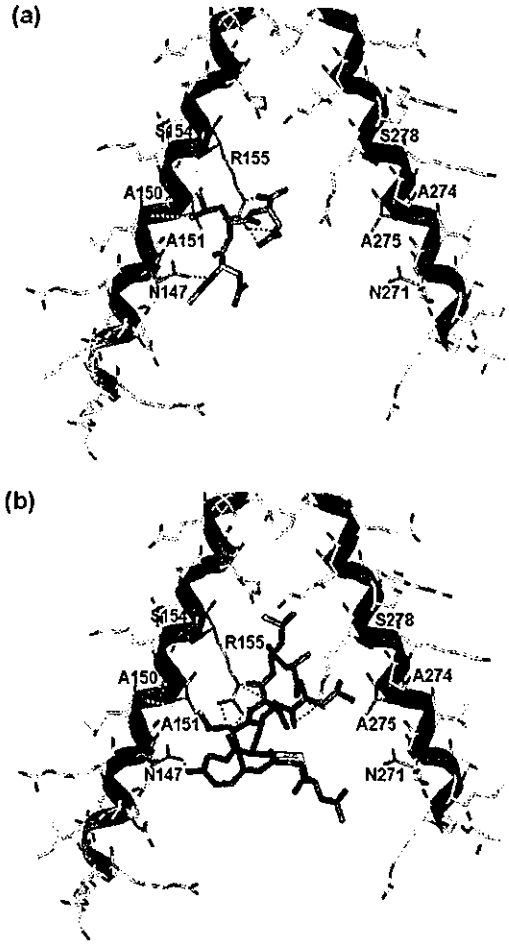

Figure 1. Docking models of the designed peptides with the binding site in the bZIP domains. (a) Ac-Asn-Leu-Asp-NH_2, pink; (b) peptide **1**, green. Ribbon representation of the Fos and Jun basic regions (c-Fos, cyan; c-Jun, magenta). Orange residues, residues involved in AP-1–DNA interactions; red broken lines, putative hydrogen bonds; yellow broken lines, putative hydrophobic interactions.

sized using the standard solid phase methodology with Fmoc chemistry and were evaluated using AP-1 binding assays in which peptides competed for the binding of digoxigenin (DIG)-labeled oligonucleotides containing the AP-1 binding site. Among these peptides, peptide **1** exhibited a weak inhibitory activity at 1 mM, whereas the corresponding linear peptide Ac-Gln-Leu-Asp-Leu-Ala-Leu-NH_2 exhibited no inhibitory activity at same concentration. It was assumed that cyclization of the flexible linear peptide converted it from an inactive to an active conformation.

Next, we performed the MD simulation of the bZIP–peptide **1** complex obtained by docking in order to relax the structure. The resulting structure of the complex from the MD simulation at 100 ps is shown in Figure 2. On the basis of the complex structure after 100 ps, we designed several cyclic peptides to interact more strongly with the putative binding site in the bZIP domains. Replacement of Leu with Asp in position 8 of peptide **1** resulted in Ac-*c*[Cys-Gly-Gln-Leu-Asp-Leu-Ala-Asp-Gly-Cys]-NH_2 (peptide **2**), which was found to possess a more potent inhibitory activity (IC_{50} = 8 μM).

We synthesized analogues of peptide **2** in which each Gly was deleted to reduce the ring size and produce more constrained cyclic decapeptides. However, each

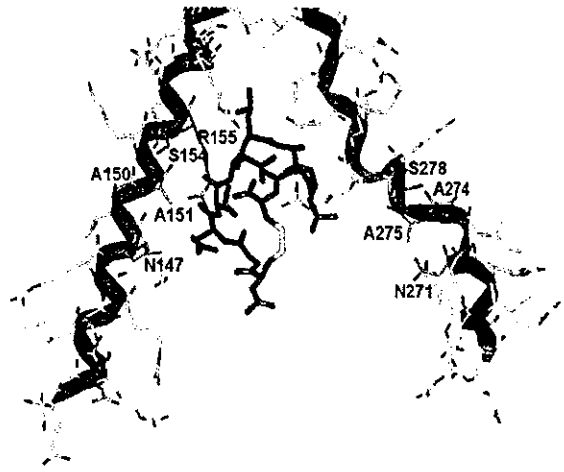

Figure 2. Snapshot taken from MD simulation of the bZIP–peptide **1** complex at 100 ps. The color coding is the same as in Figure 1.

resulting cyclic nonapeptide (Table 1; peptides **3** and **4**) demonstrated a significant loss of inhibitory activity. It was assumed that reduction of the ring size of the peptide backbone altered the peptide from an active to an inactive conformation.

Alanine Scan of Peptide 2. To evaluate the contributions of each of the amino acid side chains, we synthesized analogues of peptide **2** in which each residue, except for Cys, was substituted with Ala (Table 1; peptides **5**–**11**). This strategy has recently been used to identify the amino acid side chains participating in ligand–receptor interactions while preserving the configuration of the peptide backbone and maintaining a similar conformation.[33–36] Substitutions of Leu4, Asp5, Leu6, and Asp8 by Ala resulted in a nearly complete loss of inhibitory activities at 100 or 200 μM. Substitution of Gln3 by Ala resulted in only weak inhibitory activity. Substitution of the aspartic acid side chain in position 5 showed the greatest effect. These results indicate that side chains of Gln3, Leu4, Asp5, Leu6, and Asp8 in peptide **2** contribute significantly to inhibitory activity against the binding of AP-1 to DNA. Peptides **5** and **11**, in which each Gly residue had been substituted by Ala, were devoid of inhibitory activities. It was assumed that replacement of Gly by Ala, which is expected to restrict the conformational freedom of the peptide backbone at this point, changed the active conformation of the peptide to an inactive form.

Modification of Peptide 2. Although an alanine scan is useful for identifying important side chains, such analogues provide little information about the nature of the interactions or indirect effects due to changes in the peptide structure. To examine optimal side chains and obtain a more potent inhibitor, we synthesized analogues in which each side chain in peptide **2** was substituted with a more subtle isosteric or isoelectronic amino acid (Table 1; peptides **12**–**18**).

Gln3 was substituted with Glu or Lys (peptides **12** and **13**), resulting in complete loss of inhibitory activity at 200 μM. Substitution with Asn, causing contraction of the carboxamide side chain (peptide **14**), resulted in a moderate loss of inhibitory activity (>10-fold).

Substitution of Leu with the more hydrophobic amino acid cyclohexylalanine (Cha) (peptides **15** and **16**) resulted in a nearly complete loss of inhibitory activity.

Table 1. Analytical Data and Percentages of Inhibition at 100 μM and IC_{50} of Synthetic Peptides (**2**–**18**) of the Form Ac-c[Cys-A^2-A^3-A^4-A^5-A^6-A^7-A^8-A^9-Cys]-NH_2

peptide	sequence								MS		HPLC t_R (min)[d]		% inhibition at 100 μM	IC_{50} (μM)
	A^2	A^3	A^4	A^5	A^6	A^7	A^8	A^9	calcd[a]	obsd[b]	method 1	method 2		
2	Gly	Gln	Leu	Asp	Leu	Ala	Asp	Gly	1033.4	1033.8	11.42	8.76	81	8
3		Gln	Leu	Asp	Leu	Ala	Asp	Gly	974.4[c]	974.8[c]	11.06	9.47	−2	>100
4	Gly	Gln	Leu	Asp	Leu	Ala	Asp		974.4[c]	974.8[c]	11.12	9.72	11	>100
5	Ala	Gln	Leu	Asp	Leu	Ala	Asp	Gly	1047.4	1047.3	11.34	9.51	5	>100
6	Gly	Ala	Leu	Asp	Leu	Ala	Asp	Gly	976.4	976.8	12.36	11.10	29	>100
7	Gly	Gln	Ala	Asp	Leu	Ala	Asp	Gly	991.4	991.3	8.00	3.44	11	>100
8	Gly	Gln	Leu	Ala	Leu	Ala	Asp	Gly	989.4	989.9	10.86	8.86	−1[e]	>200
9	Gly	Gln	Leu	Asp	Ala	Ala	Asp	Gly	991.4	991.9	7.33	3.44	7	>100
10	Gly	Gln	Leu	Asp	Leu	Ala	Ala	Gly	989.4	989.9	11.38	9.85	14	>100
11	Gly	Gln	Leu	Asp	Leu	Ala	Asp	Ala	1047.4	1047.5	11.65	10.12	15	>100
12	Gly	Glu	Leu	Asp	Leu	Ala	Asp	Gly	1034.4	1034.4	11.44	10.14	−2[e]	>200
13	Gly	Lys	Leu	Asp	Leu	Ala	Asp	Gly	1033.4	1033.6	10.13	7.78	−2[e]	>200
14	Gly	Asn	Leu	Asp	Leu	Ala	Asp	Gly	1019.4	1019.8	10.55	8.34	42	>100
15	Gly	Gln	Cha	Asp	Leu	Ala	Asp	Gly	1073.4	1073.4	13.40	14.44	−22	>100
16	Gly	Gln	Leu	Asp	Cha	Ala	Asp	Gly	1073.4	1073.4	13.61	14.68	10	>100
17	Gly	Gln	Leu	Asp	Leu	Gly	Asp	Gly	1019.4	1019.4	10.32	8.31	1[e]	>200
18	Gly	Gln	Leu	Asp	Leu	Ala	Asn	Gly	1032.4	1032.8	10.93	7.72	64	52

[a] Theoretical molecular mass (M + H^+, Da) except for **3** and **4**. [b] Observed molecular mass (M + H^+, Da) except for **3** and **4**. [c] (M − H^+, Da). [d] Retention time (see Experimental Section). [e] Synthetic peptides were assayed at 100 μM except for **8**, **12**, **13**, and **17** (at 200 μM).

At these positions, Leu would be suitable for the interaction with AP-1. Substitution of Ala7 with Gly (peptide **17**) resulted in a complete loss of inhibitory activity. The methyl side chain of Ala might participate in the interaction with AP-1, or the replacement with Gly might change the active conformation of the peptide to an inactive form.

Asp8 was substituted with Asn (peptide **18**), resulting in a moderate loss of inhibitory activity (6.5-fold). At this position, the charge−charge interaction with AP-1 would be more favorable. Of the peptides tested in this study, peptide **2** emerged as that with the most potent inhibitory activity against the binding of AP-1 to DNA.

Three-Dimensional Pharmacophore Modeling. To obtain 3D structural information for the active conformation of peptide **2**, we carried out a MD simulation of the bZIP−peptide **2** complex with explicit water molecules and NMR measurements of peptide **2** in water. The MD simulation was run for 400 ps until the system was equilibrated. Six snapshots, extracted at 10 ps intervals from the last 50 ps MD simulation, were similar to one another in terms of RMS deviation for all backbone N, C_α, C, and O atoms (mean ± SD = 1.85 ± 0.48 Å). Peptide **2** was stable during the last 50 ps of the MD simulation, and the average RMS deviations between each of the six snapshots for all backbone atoms and all heavy atoms were 0.65 ± 0.17 and 0.89 ± 0.13 Å, respectively.

The binding model of peptide **2** at 400 ps is presented in Figure 3. The leucine zipper region retained approximately 70% of the α-helical conformation at the carboxyl terminal, whereas the basic regions underwent a partial change to a random coil conformation, in particular for the c-Jun domain. This is similar to information obtained by CD and NMR about the solution structure of the AP-1 or GCN4 bZIP domains in the absence of DNA.[8,9] We speculate that the binding mode of peptide **2** with the bZIP domains is different from that of its binding to DNA.

The sequence-specific NMR assignment of peptide **2** was achieved according to the standard method established by Wüthrich.[37] Identification of amino acid spin systems was based on DQF-COSY[38] and TOCSY[39] spectra and complemented with the results of NOESY[40] experiments. Starting with the unique residue Ala7, which could be easily identified on the basis of its spin type, sequential connectivities were carried out by the analysis of the $C_\alpha H_{(i)}$−$NH_{(i+1)}$ ($d_{\alpha N}$) and $NH_{(i)}$−$NH_{(i+1)}$ nuclear Overhauser effects (NOEs). Figure 4 shows the C_αH−NH fingerprint region of the NOESY spectrum containing sequential $d_{\alpha N}$ connectivities. The proton chemical shifts of peptide **2** are summarized in Table 2.

Figure 3. Binding model of peptide **2** (yellow) resulting from MD simulation at 400 ps. Ribbon representation of the bZIP domains (c-Fos, cyan; c-Jun, magenta).

For solution structure determination of peptide **2**, 12 intraresidual, 37 sequential, 19 medium range ($|i - j| < 5$, where i and j are residue numbers), and three long range ($|i - j| \geq 5$) NOEs were detected and converted to the distance constraints. On the basis of the ^3J(H-C_α-C_β-H) coupling constants and the intensities of

Table 2. ^{1}H Chemical Shifts[a] (ppm) for Peptide **2** at 5 °C and pH 4.65

residue	NH	H_α	H_β	others
CH_3[b]		2.02		
Cys1	8.62	4.64	3.00 (β2), 3.19 (β3)	
Gly2	8.89	3.95		
Gln3	8.37	4.26	1.98 (β2), 2.11 (β3)	C_γ 2.33; C_ϵ 6.92, 7.66
Leu4	8.33	4.28	1.57, 1.70	C_γ 1.57; C_δ 0.82, 0.88
Asp5	8.14	4.54	2.68, 2.84	
Leu6	8.17	4.29	1.58, 1.65	C_γ 1.57; C_δ 0.82, 0.88
Ala7	8.28	4.23	1.38	
Asp8	8.21	4.58	2.69 (β3), 2.77 (β2)	
Gly9	8.34	3.87, 4.02		
Cys10	8.25	4.60	3.00 (β2), 3.21 (β3)	
NH_2[b]	7.27, 7.77			

[a] Chemical shifts are relative to the water resonance located at 4.95 ppm. [b] Peptide **2** has an acetylated N terminus and an amidated C terminus.

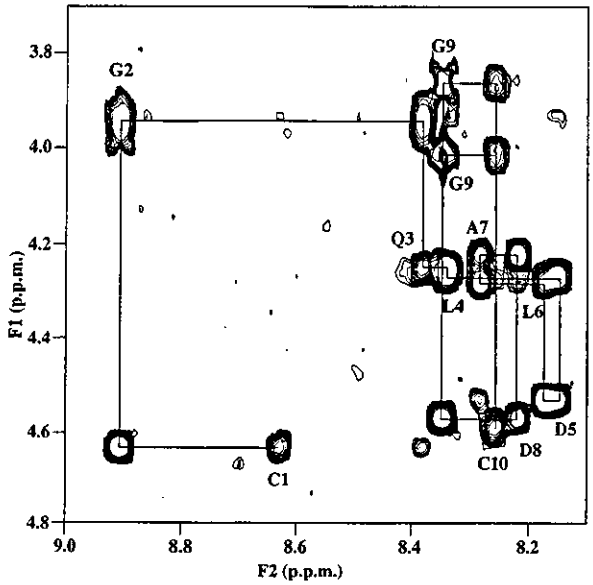

Figure 4. Sequential NOE connectivities for residues 1−10 of peptide **2** in the NOESY spectrum observed with a mixing time of 500 ms at 5 °C. Intraresidue NH-C_αH cross-peaks are labeled with the residue number by standard single-letter amino acid abbreviations.

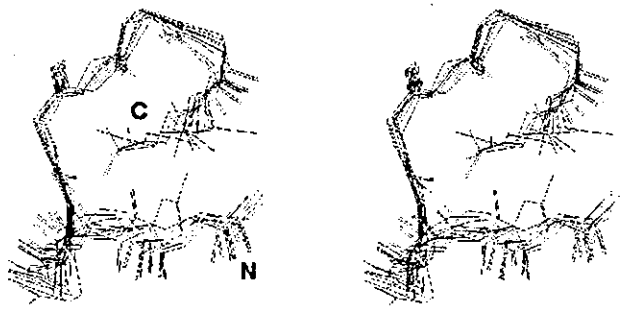

Figure 5. Stereoview of the superimposition of the 11 converged structures of the major cluster of peptide **2**. These are the results of the best fit of all backbone N, C_α, C, and O atoms.

intraresidual NOEs, we established the stereospecific assignments of the prochiral β-methylene protons and the range of the χ_1 side chain dihedral angles for Cys1, Gln3, Asp8, and Cys10. A total of 75 NMR constraints, which consisted of 71 distance constraints and four dihedral angle constraints, were used for the following simulated annealing calculations.

A set of 200 individual structures was calculated on the basis of the NMR experimental constraints. These

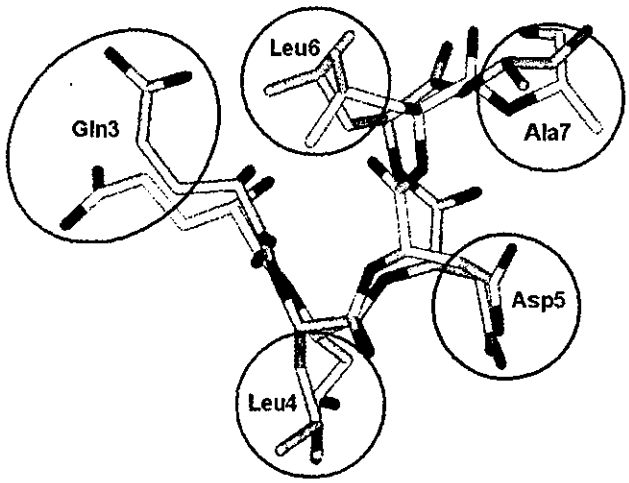

Figure 6. Superimposition of Gln3-Leu4-Asp5-Leu6-Ala7 of peptide **2** of the lowest energy conformer obtained by NMR (white) and MD simulation-derived structure at 400 ps (yellow). These are the results of the best fit of the backbone atoms. Three-dimensional pharmacophore model of AP-1 binding compounds: green, hydrophobic groups; blue, hydrogen donor or acceptor group; and red, acidic group.

calculations provided 17 structures that had no distance violations >0.2 Å and no dihedral angle violations >5°. The resulting conformations were grouped into three clusters according to the pairwise RMS deviations between 17 individual structures. Figure 5 shows a stereoview of the best-fit superimposition of the backbone atoms for the 11 individual converged structures of the major cluster. The average pairwise RMS deviation between the 11 structures was 1.18 ± 0.54 Å for all backbone atoms.

Here, we hypothesized that the rigid part of the cyclic peptide solution structure might be conserved in the biologically active conformation. Superimposition studies showed that the MD simulation-derived structures of peptide **2** in the complex were similar to the major cluster of the NMR-determined solution structures of peptide **2** in the backbones of the sequence Gln3-Leu4-Asp5-Leu6-Ala7 (1.45 ± 0.10 Å). Among these residues, the side chains of Glu3, Leu4, Asp5, and Leu6 have been shown by the alanine scan experiment to be important for inhibitory activity, as described above. Although it is unknown whether Ala7 is involved in the hydrophobic interaction with AP-1, we assumed that it contributes to the observed inhibitory activity.

From these results, we built a 3D pharmacophore model of AP-1 binding compounds, based on the chemi-

cal and structural features of the amino acid side chains of residues 3–7 in peptide **2** (Figure 6). The pharmacophore consists of three hydrophobic groups, one hydrogen bond acceptor or donor, and one acidic group. This 3D model will be useful in the process of molecular design and the search of 3D databases to identify the chemical structures of potential novel AP-1 inhibitors.

Conclusions

In the absence of precise 3D structural information about AP-1, a combination of the available experimental data and molecular modeling methods—such as docking and MD simulations—was used to design novel inhibitors of AP-1. The computer-aided molecular design strategies used in the present study produced novel cyclic decapeptides that exhibited AP-1 inhibitory activity. Such peptides will prove useful as intermediates in the search for nonpeptide and small molecule inhibitors.

This study proposes a 3D pharmacophore model of AP-1 binding compounds. We aim to use our model to discover small molecule inhibitors of AP-1 based on de novo design or 3D database searches. Although this model relies on many hypotheses and remains speculative, the current successful development of nonpeptide inhibitors lends credibility to the 3D pharmacophore model of AP-1 binding compounds.

Experimental Section

Abbreviations. Abbreviations of common amino acids and representations of peptides are in accordance with the recommendations of the IUPAC-IUB Joint Commission on Biochemical Nomenclature.[41] Additional abbreviations are used as follows: DMF, *N*,*N*-dimethylformamide; DMSO, dimethyl sulfoxide; Fmoc, 9-fluorenylmethoxycarbonyl; HPLC, high-performance liquid chromatography; mequiv, milliequivalent; *t*Bu, *tert*-butyl; TFA, trifluoroacetic acid; Trt, triphenylmethyl.

Materials and Methods. Rink Amide MBHA resin (0.55 mequiv/g) was obtained from NovaBiochem (Läufelfingen, Switzerland). All of the protected amino acids (Fmoc and Fmoc plus Trt or *t*Bu) and the coupling reagents were purchased from NovaBiochem. All purchased amino acids were of the L-configuration. All reagents and solvents were reagent grade or better and were used without further purification.

HPLC was performed with a Hitachi L-7100 apparatus equipped with an L-7400 UV detector (peak detection at 230 nm) using an ODS-AP column (YMC-Pack, YMC Co., Kyoto, Japan) of 250 mm × 20 mm for preparative or 150 mm × 4.6 mm for analytical HPLC, respectively. Liquid chromatography–electrospray ionization mass spectrometry was performed with a Finnigan 700 triple-sector quadrupole mass spectrometer equipped with a Waters 626 LC system and a Finnigan MAT electrospray ionization system (4.5 kV).

Peptide Synthesis. All peptides were synthesized manually using standard solid phase peptide chemistry[42] with Fmoc-protected amino acids[43] on Rink Amide MBHA resin[44] at a 0.2 mmol scale. Couplings with Fmoc amino acids (3 equiv) were performed in the presence of 1-hydroxybenzotriazole and 1,3-diisopropylcarbodiimide (each 3 equiv) in DMF (5 mL) at room temperature for 2 h, and then, the Fmoc protecting group was removed by treatment with 20% piperidine in DMF (5 mL) at room temperature for 20 min. After deprotection of the last Fmoc group on Cys(Trt), the peptide resin was treated with acetic anhydride and *N*,*N*-diisopropylethylamine (each 10 equiv) in a 1:1 mixture of DMF and CH_2Cl_2 (5 mL) at room temperature for 30 min before filtration and washing with DMF (×4) and CH_2Cl_2 (×3) followed by drying in vacuo. The terminal-N-acetyl product was treated with a mixture of TFA–thioanisole–water (92.5:5.0:2.5) (20 mL) at room temperature for 4 h to induce cleavage of the peptide from the resin and removal of the remaining O- and S-protecting groups. The exhausted resin was filtered, the filtrate was mixed with ether (50 mL), and the precipitate was isolated by centrifugation.

A solution of the dithiol product in 10% DMSO in TFA (10 mL) was stirred at room temperature for 20 h before concentration to approximately 2 mL and the addition of ether (50 mL).[45] The precipitate was collected by centrifugation and purified by preparative reverse phase HPLC eluted with a linear gradient of acetonitrile in water containing 0.1% TFA at a flow rate of 8.0 mL/min before lyophilization. The homogeneity of the resulting peptides was tested by analytical HPLC using two solvent systems: method 1, 30 min gradient of 10–70% acetonitrile in 0.1% aqueous TFA; method 2, 30 min gradient of 35–95% methanol in 0.1% aqueous TFA. The purity of the peptides was determined by HPLC to be >95%. A summary of the analytical results for each peptide described in this paper is provided in Table 1.

Enzyme-Linked DNA–Protein Interaction Assay. The inhibition constants of the synthetic peptides for DNA binding activity of AP-1 were determined by an enzyme-linked DNA–protein interaction assay using synthetic double-stranded oligonucleotides, which contain the AP-1 binding site (shown in bold) and nuclear protein. The synthetic oligonucleotides 5′-CTAGTGA**TGAGTCA**GCCGGATC-3′ and 5′-GATCCGGC-**TGACTCA**TCACTAG-3′ (Bio-Synthesis, Lewisville, TX) were labeled with DIG-ddUTP as described in the DIG oligonucleotide 3′-end-labeling kit (Boehringer Mannheim, Mannheim, Germany). After they were annealed, they were used as DIG-labeled double-stranded oligonucleotides. Nuclear extract proteins were prepared from phorbol myristate acetate-stimulated HeLa cells according to the protocol described by Dignam et al.[46] and were used after dialysis against reaction buffer [20 mM *N*-(2-hydroxyethyl)piperazine-*N*′-2-ethanesulfonic acid-KOH (pH 7.9) containing 0.5 mM ethylenediaminetetraacetic acid, 50 mM KCl, 0.5 mM dithiothreitol, 0.5 mM phenylmethylsulfonyl fluoride, and 10% (v/v) glycerol].

Ninety-six well microplates (Corning Inc., Corning, NY) were coated with nuclear extract (1 μg/mL; 100 μL/well) at 4 °C overnight. After they were washed with phosphate-buffered saline containing 0.05% Tween-20, DIG-labeled double-stranded oligonucleotides (10 pM) in reaction buffer were mixed with each sample dissolved in DMSO (99:1–98:2), and 100 μL of each mixture was added to the wells. After they were incubated for 1 h at room temperature, the wells were washed with reaction buffer containing 0.05% Tween-20. Horseradish peroxidase-conjugated goat anti-DIG antibody (0.04 units/mL, Boehringer Mannheim) in binding buffer containing 0.1% bovine serum albumin was added (100 μL/well) and incubated for 1 h at room temperature. *o*-Phenylenediamine (1 mg/mL) in 100 mM Na_2HPO_4/200 mM citric acid buffer (pH 5.0) containing 0.1% H_2O_2 was added (100 μL/well), and the color reaction was allowed to develop for 20 min at room temperature. After 50 μL of 1 M H_2SO_4 was added to each well to stop the reaction, the optical density was measured with a microplate reader (Bio-Rad model 450, Bio-Rad Laboratories, Hercules, CA) at a wavelength of 492 nm. The IC_{50} values were calculated by a logistic concentration–response curve using the SAS System version 8.2 (SAS Institute Inc., Cary, NA).

NMR Measurements and Simulated Annealing Calculations. Peptide **2** (4 mg) was dissolved in 0.5 mL of either 90% H_2O/10% D_2O or D_2O containing 50 mM CD_3COONa. The sample solution was adjusted to pH 4.65. All NMR spectra were recorded on a Varian INOVA600 spectrometer operating at 600 MHz for a proton frequency at two temperatures: 5 and 25 °C. For spectral assignment and extraction of structural information, DQF-COSY,[38] TOCSY,[39] NOESY,[40] ROESY,[47] and E.COSY[48] experiments were performed in the phase sensitive mode.[49] The DQF-COSY and E.COSY spectra were recorded with 512 increments of 8K data points and 32 transients. The TOCSY spectra were recorded with mixing times of 20 and 50 ms. The NOESY spectra were obtained with mixing times of 100, 200, 300, and 500 ms at 5 °C. The ROESY spectrum was obtained with a mixing time of 500 ms at 5 and 25 °C. Five

hundred twelve increments of 2K data points were recorded with 32–96 transients for the TOCSY, NOESY, and ROESY experiments. The solvent resonance was suppressed by selective irradiation during a relaxation delay of 2.0 s. The ^3J(H-C_α-C_β-H) measurement was carried out on an E.COSY spectrum recorded in D_2O. The chemical shifts were referenced with respect to H_2O, which in turn was calibrated using an internal standard, 2,2-dimethyl-2-silapentane-5-sulfonate, in a different sample. The chemical shift values of 4.95 and 4.75 ppm for the water signal were used at temperatures of 5 and 25 °C, respectively.

Interproton distance constraints were obtained from the NOESY spectra. Spin-diffusion effects were inspected by following the buildup of NOESY cross-peaks when mixing times were increased from 100 to 500 ms. The distance constraints were classified into four categories corresponding to 1.8–2.7, 1.8–3.5, 1.8–5.0, and 1.8–6.0 Å. Pseudoatoms were used for the prochiral methylene protons that had not been assigned in a stereospecific way, the methyl groups of the Ala and Leu residues and the C_α proton of the Gly residues.[50] Correction factors for the use of pseudoatoms were added to the distance constraints. In addition, 0.5 Å was added to the distance constraints involving methyl protons. All calculations were performed on a Silicon Graphics Octane workstation with the X-PLOR program.[51] The dynamical simulated annealing protocols were used to calculate the 3D structures.

Acknowledgment. This study was partially supported by the Japan Science and Technology Agency.

References

(1) Angel, P.; Karin, M. The Role of Jun, Fos and the AP-1 Complex in Cell-Proliferation and Transformation. *Biochim. Biophys. Acta* **1991**, *1072*, 129–157.
(2) Foletta, V. C.; Segal, D. H.; Cohen, D. R. Transcriptional Regulation in the Immune System: All Roads Lead to AP-1. *J. Leukocyte Biol.* **1998**, *63*, 139–152.
(3) Angel, P.; Baumann, I.; Stein, B.; Delius, H.; Rahmsdorf, H. J.; Herrlich, P. 12-*O*-Tetradecanoyl-Phorbol-13-Acetate Induction of the Human Collagenase Gene Is Mediated by an Inducible Enhancer Element Located in the 5′-Flanking Region. *Mol. Cell. Biol.* **1987**, *7*, 2256–2266.
(4) Suto, M. J.; Ransone, L. J. Novel Approaches for the Treatment of Inflammatory Diseases: Inhibitors of NF-κB and AP-1. *Curr. Pharm. Des.* **1997**, *3*, 515–528.
(5) Shiozawa, S.; Shimizu, K.; Tanaka, K.; Hino, K. Studies on the Contribution of c-fos/AP-1 to Arthritic Joint Destruction. *J. Clin. Invest.* **1997**, *99*, 1210–1216.
(6) Kouzarides, T.; Ziff, E. The Role of the Leucine Zipper in the Fos-Jun Interaction. *Nature* **1988**, *336*, 646–651.
(7) Glover, J. N. M.; Harrison, S. C. Crystal Structure of the Heterodimeric bZIP Transcription Factor c-Fos-c-Jun Bound to DNA. *Nature* **1995**, *373*, 257–261.
(8) Patel, L.; Abate, C.; Curran, T. Altered Protein Conformation on DNA Binding by Fos and Jun. *Nature* **1990**, *347*, 572–575.
(9) Saudek, V.; Pastore, A.; Morelli, M. A. C.; Frank, R.; Gausepohl, H.; Gibson, T.; Weih, F.; Roesch, P. Solution Structure of the DNA-Binding Domain of the Yeast Transcriptional Activator Protein GCN4. *Protein Eng.* **1990**, *4*, 3–10.
(10) Gohlke, H.; Klebe, G. Approaches to the Description and Prediction of the Binding Affinity of Small-Molecule Ligands to Macromolecular Receptors. *Angew. Chem., Int. Ed.* **2002**, *41*, 2644–2676.
(11) Davis, A. M.; Teague, S. J.; Kleywegt, G. J. Application and Limitations of X-ray Crystallographic Data in Structure-Based Ligand and Drug Design. *Angew. Chem., Int. Ed.* **2003**, *42*, 2718–2736.
(12) Lee, S.; Park, S.; Jun, G.; Hahm, E.-R.; Lee, D.-K.; Yang, C.-H. Quantitative Assay for the Binding of Jun-Fos Dimer and Activator Protein-1 Site. *J. Biochem. Mol. Biol.* **1999**, *32*, 594–598.
(13) Hahm, E.-R.; Cheon, G.; Lee, J.; Kim, B.; Park, C.; Yang, C.-H. New and Known Symmetrical Curcumin Derivatives Inhibit the Formation of Fos-Jun-DNA Complex. *Cancer Lett.* **2002**, *184*, 89–96.
(14) Park, S.; Lee, D.-K.; Yang, C.-H. Inhibition of Fos-Jun-DNA Complex Formation by Dihydroguaiaretic Acid and in Vitro Cytotoxic Effects on Cancer Cells. *Cancer Lett.* **1998**, *127*, 23–28.
(15) Park, S.; Lee, D. K.; Whang, Y. H.; Yang, C. H. Momordin I, a Compound of Ampelopsis Radix, Inhibits AP-1 Activation Induced by Phorbol Ester. *Cancer Lett.* **2000**, *152*, 1–8.
(16) Goto, M.; Masegi, M.; Yamauchi, T.; Chiba, K.; Kuboi, Y.; Harada, K.; Naruse, N. K1115 A, a New Anthraquinone Derivative that Inhibits the Binding of Activator Protein-1 (AP-1) to its Recognition Sites. *J. Antibiot.* **1998**, *51*, 539–544.
(17) Ghose, A. K.; Wendoloski, J. J. Pharmacophore Modelling: Methods, Experimental Verification and Applications. *Perspect. Drug Discovery Des.* **1998**, 253–271.
(18) Hruby, V. J. Conformational and Topographical Considerations in the Design of Biologically Active Peptides. *Biopolymers* **1993**, *33*, 1073–1082.
(19) Li, P.; Roller, P. P. Cyclization Strategies in Peptide Derived Drug Design. *Curr. Top. Med. Chem.* **2002**, *2*, 325–341.
(20) *SYBYL 6.4*; Tripos, Inc.: St. Louis, MO, 1997.
(21) Nakabeppu, Y.; Nathans, D. The Basic Region of Fos Mediates Specific DNA Binding. *EMBO J.* **1989**, *8*, 3833–3841.
(22) Turner, R.; Tjian, R. Leucine Repeats and an Adjacent DNA Binding Domain Mediate the Formation of Functional cFos-cJun Heterodimers. *Science* **1989**, *243*, 1689–1694.
(23) Gentz, R.; Rauscher, F. J., III; Abate, C.; Curran, T. Parallel Association of Fos and Jun Leucine Zippers Juxtaposes DNA Binding Domains. *Science* **1989**, *243*, 1695–1699.
(24) Neuberg, M.; Schuermann, M.; Hunter, J. B.; Müller, R. Two Functionally Different Regions in Fos are Required for the Sequence-Specific DNA Interaction of the Fos/Jun Protein Complex. *Nature* **1989**, *338*, 589–590.
(25) Risse, G.; Jooss, K.; Neuberg, M.; Brüller, H.-J.; Müller, R. Asymmetrical Recognition of the Palindromic AP1 Binding Site (TRE) by Fos Protein Complexes. *EMBO J.* **1989**, *8*, 3825–3832.
(26) Ransone, L. J.; Visvader, J.; Wamsley, P.; Verma, I. M. Trans-Dominant Negative Mutants of Fos and Jun. *Proc. Natl. Acad. Sci. U.S.A.* **1990**, *87*, 3806–3810.
(27) Clark, M.; Cramer, R. D, III; Van Opdenbosch, N. Validation of the General Purpose Tripos 5.2 Force Field. *J. Comput. Chem.* **1989**, *10*, 982–1012.
(28) Gasteiger, J.; Marsili, M. Iterative Partial Equalization of Orbital Electronegativity—A Rapid Access to Atomic Charges. *Tetrahedron* **1980**, *36*, 3219–3228.
(29) Purcell, W. P.; Singer, J. A. A Brief Review and Table of Semiempirical Parameters Used in the Hückel Molecular Orbital Method. *J. Chem. Eng. Data* **1967**, *12*, 235–246.
(30) Pearlman, D. A.; Case, D. A.; Caldwell, J. W.; Ross, W. S.; Cheatham, T. E., III; Ferguson, D. M.; Seibel, G. L.; Singh, U. C.; Weiner, P.; Kollman, P. A. *AMBER 4.1*; University of California: San Francisco, CA, 1995.
(31) Jorgensen, W. L.; Chandrasekhar, J.; Madura, J. D.; Impey, R. W.; Klein, M. L. Comparison of Simple Potential Functions for Simulating Liquid Water. *J. Chem. Phys.* **1983**, *79*, 926–935.
(32) Ryckaert, J.-P.; Ciccotti, G.; Berendsen, H. J. C. Numerical Integration of the Cartesian Equations of Motion of a System with Constraints: Molecular Dynamics of *n*-Alkanes. *J. Comput. Phys.* **1977**, *23*, 327–341.
(33) Peeters, T. L.; Macielag, M. J.; Depoortere, I.; Konteatis, Z. D.; Florance, J. R.; Lessor, R. A.; Galdes, A. D-Amino Acid and Alanine Scans of the Bioactive Portion of Porcine Motilin. *Peptides* **1992**, *13*, 1103–1107.
(34) Tam, J. P.; Liu, W.; Zhang, J.-W.; Galantino, M.; Bertolero, F.; Cristiani, C.; Vaghi, F.; De Castiglione, R. Alanine Scan of Endothelin: Importance of Aromatic Residues. *Peptides* **1994**, *15*, 703–708.
(35) Sahm, U. G.; Olivier, G. W. J.; Branch, S. K.; Moss, S. H.; Pouton, C. W. Synthesis and Biological Evaluation of α-MSH Analogues Substituted with Alanine. *Peptides* **1994**, *15*, 1297–1302.
(36) Leprince, J.; Gandolfo, P.; Thoumas, J.-L.; Patte, C.; Fauchère, J.-L.; Vaudry, H.; Tonon, M.-C. Structure–Activity Relationships of a Series of Analogues of the Octadecaneuropeptide ODN on Calcium Mobilization in Rat Astrocytes. *J. Med. Chem.* **1998**, *41*, 4433–4438.
(37) Wüthrich, K. *NMR of Proteins and Nucleic Acids*; John Wiley & Sons: New York, 1986.
(38) Rance, M.; Sørensen, O. W.; Bodenhausen, G.; Wagner, G.; Ernst, R. R.; Wüthrich, K. Improved Spectral Resolution in COSY ^{1}H NMR Spectra of Proteins via Double Quantum Filtering. *Biochem. Biophys. Res. Commun.* **1983**, *117*, 479–485.
(39) Bax, A.; Davis, D. G. MLEV-17-Based Two-Dimensional Homonuclear Magnetization Transfer Spectroscopy. *J. Magn. Reson.* **1985**, *65*, 355–360.
(40) Macura, S.; Huang, Y.; Suter, D.; Ernst, R. R. Two-Dimensional Chemical Exchange and Cross-Relaxation Spectroscopy of Coupled Nuclear Spins. *J. Magn. Reson.* **1981**, *43*, 259–281.
(41) IUPAC-IUB Joint Commission on Biochemical Nomenclature (JCBN) Nomenclature and Symbolism for Amino Acids and Peptides. *J. Biol. Chem.* **1985**, *260*, 14–42.
(42) Merrifield, R. B. Solid Phase Peptide Synthesis. I. The Synthesis of a Tetrapeptide. *J. Am. Chem. Soc.* **1963**, *85*, 2149–2154.

Materials and methods

Cell culture. Samples of synovium were obtained during joint surgery from patients with RA and osteoarthritis (OA), following the world medical association declaration of Helsinki ethical principles for medical research involving human subjects. The diagnosis of RA was made according to the 1987 revised criteria of American College of Rheumatology (18). Tissues were minced and digested in a solution containing 0.2% of collagenase (Sigma, St. Louis, MO) and 0.25% of trypsin-ethylenediamine tetraacetic acid (trypsin-EDTA; DifcoI Laboratories, Detroit, MI) at 37°C for 1 h. Dispersed rheumatoid synovial cells were cultured in a 10 cm dish (Asahi Techno Glass Corp., Tokyo, Japan) with DMEM (Nissui Pharmaceutical Co., Ltd., Tokyo, Japan) containing 10% FCS (Biosciences Pty Ltd., Lome, Australia) supplemented with 50 U/ml penicillin and 50 µg/ml streptomycin. After overnight culture, non-adherent cells were removed, and adherent cells were further incubated in fresh medium. All experiments were conducted using the cells of 3-4 passage.

Preparation of nuclear extracts. Synovial cells ($3x10^5$) were treated with ~100 nM of geldanamycin (Sigma-Aldrich, St. Louis, MO), ~10 nM of radicicol (Sigma-Aldrich) or ~100 nM of herbimycin A (Sigma-Aldrich) for 12 h. The cells were cultured with 4 ng/ml of IL-1ß (Roche Diagnostics, Manheim, Germany) or 20 ng/ml of TNFα R&D systems Inc., Minneapolis, MN) for ~24 h. After washing, they were suspended in 200 µl of hypotonic buffer (10 mM HEPES-KOH, pH 7.9, 1.5 mM $MgCl_2$, 10 mM KCl, 0.5 mM DTT, 0.5 mM PMSF, 1 µM leupeptin and 1 µM aprotinin). After adding 2 µl of 10% Nonidet P-40, cells were incubated on ice for 10 min and centrifuged at 2,000 g for 30 sec, and the fraction containing nuclei was precipitated. The nuclear fraction was reacted with 50 µM of extraction buffer (20 mM HEPES-KOH, pH 7.9, 10% glycerol, 420 mM NaCl, 1.5 mM $MgCl_2$, 0.2 mM EDTA, 0.5 mM DTT, 0.5 mM PMSF, 1 µM leupeptin and 1 µM aprotinin) on ice with agitation for 30 min. The supernatant obtained after centrifugation at 15,000 g for 5 min was stored in aliquots at -80°C (nuclear extract).

Electrophoretic mobility shift assay (EMSA). Nuclear extract (5 µg) was reacted for 30 min with 0.5 pmol of digoxigenin (DIG)-labeled double-stranded AP-1 oligonucleotide probe (5'-GGCTTGATGACTCAGCCGGAA-3' and 3'-GCGAAC TACTGAGTCGGCCTT-5') in a 20 µl reaction containing 20 mM HEPES-KOH, pH 7.9, 10% glycerol, 20 mM KCl, 0.5 mM EDTA, 0.5 mM DTT, 0.5 mM PMSF, 1 µg of BSA and 0.5 µg of poly (dI-dC) (Amersham Bioscience, Piscataway, NJ). The probes were end-labeled with DIG-11-ddUTP (Roche). Supershift assay was performed by adding 1 µg of anti-Fos Ab (sc-235; Santa-Cruz Biotechnology, Santa Cruz, CA), anti-c-Jun Ab (Ab-2: Oncogene Science, Uniondale, NY), anti-JunB Ab (sc-46; Santa Cruz), or anti-JunD Ab (sc-74; Santa Cruz). Samples were run on a 4% polyacrylamide gel using 1X TGE buffer (50 mM Tris, 380 mM grycine and 2 mM EDTA), and transferred to a positively charged nylon membrane (Roche). DIG-labeled oligonucleotides were visualized by incubating with alkaline phosphatase-labeled $F(ab)_2$ anti-DIG antibodies, followed by chemiluminescence reaction with 100 µg/ml CSPD substrates (Tropix, Inc., Bedford, MA).

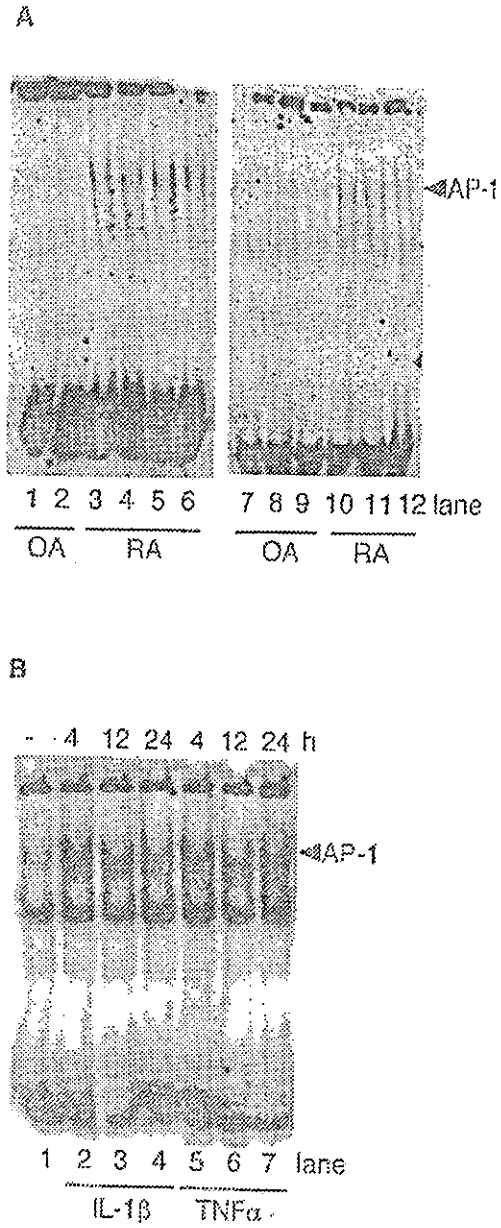

Figure 1. AP-1 binding activity in rheumatoid synovial cells. (A) EMSA for AP-1 binding comparing the nuclear extracts of synovial cells of patients with rheumatoid arthritis (RA) (n=7) and osteoarthritis (OA) (n=5). (B) EMSA for AP-1 binding under stimulation with inflammatory cytokines. Cultured rheumatoid synovial cells ($3x10^5$) stimulated with 10 ng/ml of IL-1ß (lanes 2-4) or 20 ng/ml of TNFα (lanes 5-7) for 4, 12 or 24 h were used. The data represent 4 independent experiments.

Western blotting. Cell lysates were separated using 5-15% SDS-PAGE and transferred to Immobilon-P membrane (Millipore, Bedford, MA). After blocking with 5% skim milk, the membrane was incubated with rabbit IgG anti-HSP90 Ab (sc-7947; Santa Cruz), anti-Fos Ab (Santa Cruz), anti-JunD Ab (Santa Cruz) for 2 h. The membrane was then reacted with horseradish peroxidase-conjugated anti-rabbit Ig Ab (NA934; Amersham Bioscience) and bound antibodies were visualized using the ECL system (Amersham Bioscience).

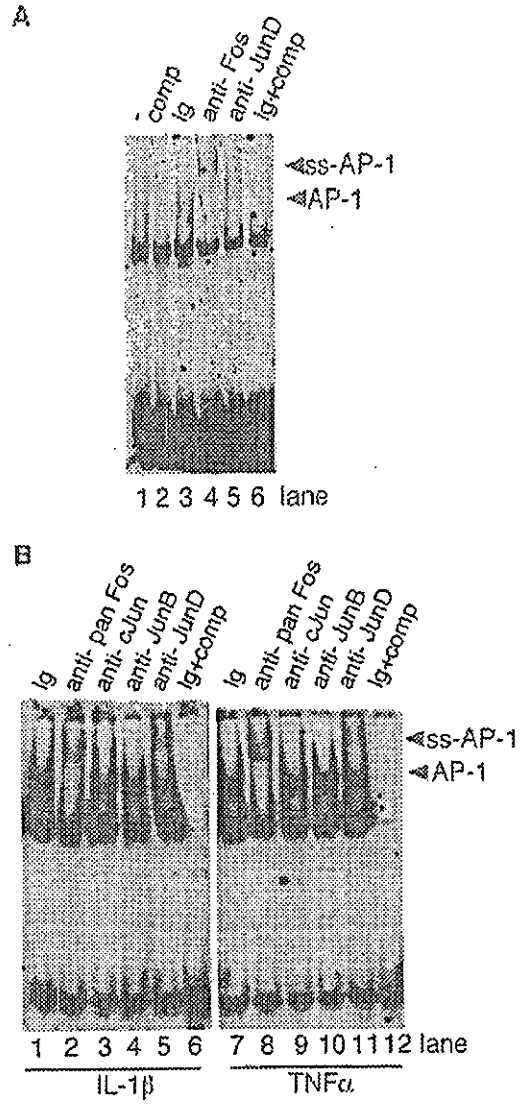

Figure 2. Supershift experiment for AP-1 in rheumatoid synovial cells. (A) Supershift experiment using specific antibodies, and competition experiment (comp) using unlabeled oligonucleotides. The bands for AP-1 and supershifted (SS) AP-1 shown with arrowheads. The data represent 5 independent experiments. (B) Supershift experiment under cytokine stimulation. The nuclear extracts obtained 6 h after stimulation with IL-1ß (lanes 1-6) or TNFα (lanes 7-12) were reacted with specific antibodies for supershift experiments. Competition assays in lanes 6 and 12. The data represent 5 independent experiments.

Results

AP-1 binding activity in RA synovial cells. The AP-1 binding activity in the nuclear extracts of rheumatoid synovial cells was compared with those of patients with OA. EMSA indicated that all 7 patients with RA showed AP-1 binding activity, whereas almost no binding was observed in patients with OA (Fig. 1A).

AP-1 binding activity is increased by inflammatory cytokines. Rheumatoid synovial cells were stimulated with inflammatory cytokines including IL-1ß and TNFα or left untreated for various time periods (4, 12, and 24 h), and the AP-1 binding activity was measured by EMSA. The AP-1 binding activity in rheumatoid synovial cells was significantly increased after stimulation with IL-1ß or TNFα (Fig.1B). The AP-1 binding peaked at 4 h and was then increased at least until 24 h after stimulation.

Supershift of Fos and JunD. Supershift experiments for AP-1 family members in the nuclear extracts of untreated or cytokine-stimulated rheumatoid synovial cells were performed using anti-Fos, anti-c-Jun, anti-JunB, and anti-JunD Abs. While only the supershift for c-Fos was observed under unstimulated conditions (Fig. 2A), supershift for both Fos and JunD proteins was observed after cytokine stimulation (Fig. 2B).

Suppression of AP-1 binding activity by specific inhibitors of HSP90. Rheumatoid synovial cells were treated either with 10 and 100 nM of geldanamycin, 1 and 10 nM of radicicol, or 10 and 100 nM of herbimycin A, and the cells were cultured with 20 ng/ml of TNFα for 6 h. The AP-1 binding activity was then compared. EMSA showed that pretreatment with as low as 10 nM of geldanamycin suppressed the increase of AP-1 binding activity in rheumatoid synovial cells (Fig. 3A, lane 3 and 4). Western blot experiments showed that the amount of cellular HSP90, Fos and JunD proteins remained unchanged irrespective of the treatments with 10 or 100 nM of geldanamycin (Fig. 4A and B, lanes 2 and 3). Further, AP-1 binding activity was also specifically inhibited by 10 nM of radicicol (Fig. 3B, lane 4) or 100 nM of herbimycin A (Fig. 3B, lane 6), while HSP90 was not decreased by the treatments (Fig. 4B).

Discussion

The results showed that AP-1 binding activity was basically higher and was further up-regulated in rheumatoid synovial cell upon stimulation with IL-1ß or TNFα, ubiquitous inflammatory cytokines elevated in sera and joint fluids of rheumatoid patients (19,20). The finding is in line with previous findings of up-regulation of c-Fos/AP-1 in arthritic disease conditions such as RA (6,21,22). As to protein composition of AP-1 dimer, we found that JunD, but not c-Jun or JunB, was specifically increased in conjunction with Fos under inflammatory cytokine stimulation, and that Fos homodimer was the major component of the AP-1 in unstimulated rheumatoid synovial cells. Previous studies have shown that c-Fos was the major component of Fos protein expressed in RA (23). Further, JunB and JunD are two major subtypes of Jun family members expressed in T cells (24,25), in which JunD is particularly expressed constantly in the cells (26). JunD is also the major component of Jun family members found in chondrocytes. JunD RNA is expressed in rheumatoid synovial cells (27). While JunD homodimer and JunB homodimer both act rather inhibitorily (28,29), Fos/JunD heterodimer has been shown to be functionally active (30,31).

We found that DNA binding activity of AP-1 was specifically inhibited by geldanamycin and other specific inhibitors of HSP90 including radicicol or herbimycin A in rheumatoid synovial cells. Further, we found that the amount of HSP90 was not decreased by the treatment with geldanamycin. Since geldanamycin specifically inhibits the function of HSP90 (14,17), it appears that functional activity, but not mere

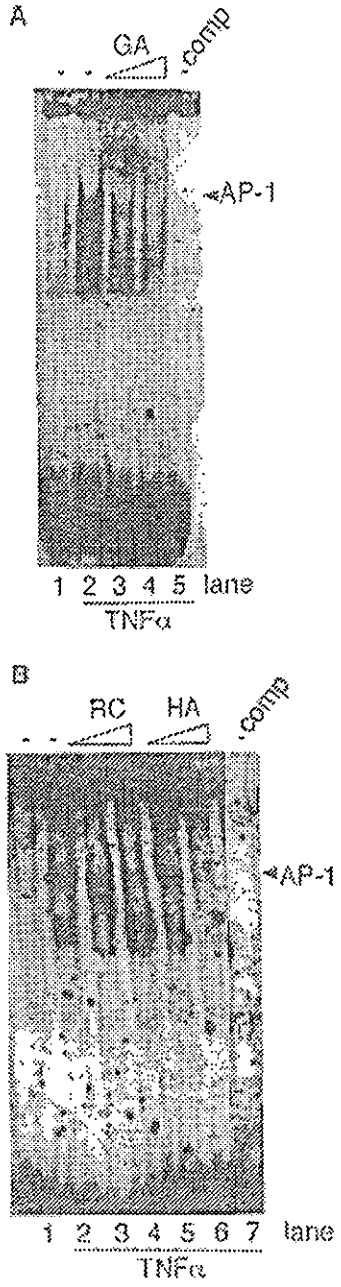

Figure 3. EMSA for AP-1 binding activity with HSP90 specific inhibitors in rheumatoid synovial cells. (A) EMSA for AP-1 binding and inhibitor geldanamycin treatment in rheumatoid synovial cells. Cultured synovial cells ($3x10^5$) were treated with 10 nM (lane 3), 100 nM (lane 4) of geldanamycin (GA), inhibitor of chaperon function of HSP90, for 12 h or left untreated (lanes 1 and 2). Cells were subsequently stimulated with 20 ng/ml of TNFα for 6 h (lanes 2-5). Competition assays done by unlabeled oligonucleotides (lane 5). The data represent 5 independent experiments. (B) EMSA for AP-1 binding and inhibitors radicicol and herbimycin A in rheumatoid synovial cells. Cultured synovial cells ($3x10^5$) were treated with 1 nM (lane 3) or 10 nM (lane 4) of radicicol (RC), 10 nM (lane 5) or 100 nM (lane 6) of herbimycin A (HA) for 12 h or left untreated. Cells were subsequently stimulated with 20 ng/ml of TNFα for 6 h (lanes 2-6). The data represent 5 independent experiments.

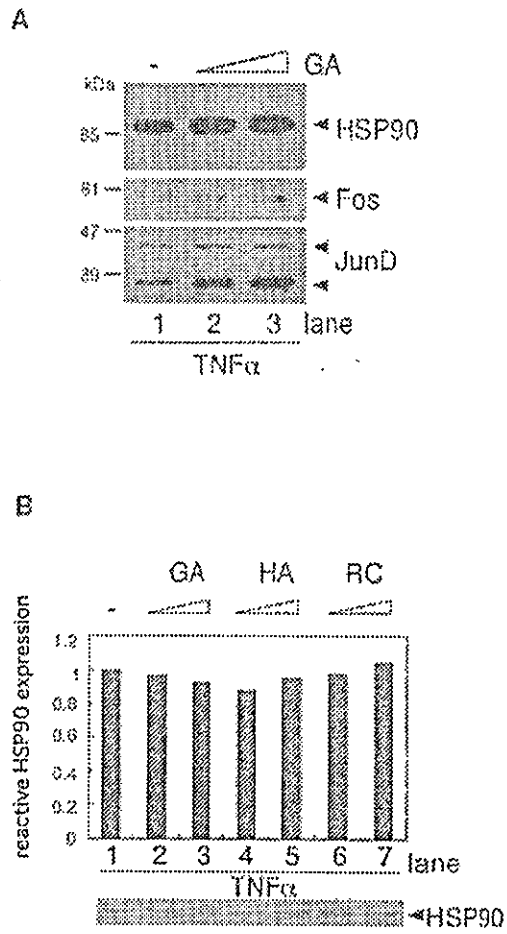

Figure 4. Western blotting for AP-1 and HSP90 with HSP90 specific inhibitors in rheumatoid synovial cells. (A) Western blotting for HSP90, Fos, and JunD proteins. Cultured RA synovial cells were treated with 10 nM (lane 2) or 100 nM (lane 3) of geldanamycin for 12 h or left untreated (lane 1). Cells were subsequently stimulated with 20 ng/ml TNFα for 6 h. Cell extracts assayed by Western blotting using anti-HSP90 Ab (upper panel), anti-Fos Ab (middle panel), or anti-JunD Ab (lower panel). The figure represents 4 independent experiments using different rheumatoid synovial cells. (B) Western blotting for HSP90 with inhibitors, geldanamycin, radicicol, and herbimycin A, in rheumatoid synovial cells. Cultured RA synovial cells were treated with 10 nM (lane 2) or 100 nM (lane 3) of geldanamycin (GA), 10 nM (lane 4) or 100 nM (lane 5) of herbimycin A (HA), or 1 nM (lane 6) or 10 nM (lane 7) of radicicol (RC) for 12 h or left untreated (lane 1). Cells were subsequently stimulated with 20 ng/ml of TNFα for 6 h. HSP90 expression was quantified by densitometry and compared (upper graph). The data represent 2 independent experiments.

presence, of HSP90 is required for AP-1 binding in rheumatoid synovial cells. Previous studies have shown that one of the major inflammatory cytokines, IL-6, up-regulates transactivation of HSP90 (32) and that IgG antibody against HSP90 is detectable in rheumatoid patients with joint erosion (33). Further, geldanamycin suppresses progression of adjuvant-induced arthritis (34). Thus, it is likely that HSP90 modulates transactivation of the genes such as IL-1ß, IL-6, TNFα and matrix metalloproteinases indirectly through AP-1 binding (35).

Previous studies have shown that HSP90 does not increase the amount of AP-1 proteins in human lung carcinoma A549 cells when stimulated with TNFα or phorbol 12-myristate 13-acetate (35). However, HSP90 up-regulated the DNA binding activity, i.e., the function of AP-1 (Fos/JunD). While JunD was composed of two isoforms, 38 and 43 kDa, as deduced from two different translational start codons contained in *JunD* gene as found in this and other studies (36), we found that the amounts of JunD and Fos was unchanged or rather slightly increased by the treatment with geldanamycin (Fig. 2B). Thus, geldanamycin appears to inhibit AP-1

binding activity by functionally inactivating HSP90. While the relationship between AP-1 protein and geldanamycin in relation to HSP90 has been pointed out in the literature (35), the evidence obtained so far did not indicate that HSP90 directly bind AP-1. Molecular mechanism of the action of HSP90 on AP-1 should be clarified in future.

Acknowledgements

This study was supported in part by the grant-in-aid for scientific research (A) 09470127 and (B) 11557026 the grant for 21st Century COE program, 'Center of Excellence for Signal Transduction Disease: Diabetes Mellitus as Model' from Ministry of Education, Culture, Sports, Science and Technology of Japan to S.S. S.S. is the investigator of the center of excellence (COE) Japan.

References

1. Tak PP and Bresnihan B: The pathogenesis and prevention of joint damage in rheumatoid arthritis: advances from synovial biopsy and tissue analysis. Arthritis Rheum 43: 2619-2633, 2000.
2. Shiozawa S, Tanaka Y, Fujita T and Tokuhisa T: Destructive arthritis without lymphocyte infiltration in H2-c-fos transgenic mice. J Immunol 148: 3100-3104, 1992.
3. Kuroki Y, Shiozawa S, Sugimoto T and Fujita T: Constitutive expression of c-fos gene inhibits type 1 collagen synthesis in transfected osteoblasts. Biochem Biophys Res Commun 182: 1389-1394, 1992.
4. Kuroki Y, Shiozawa S, Yoshihara R and Hotta H: The contribution of human c-fos DNA to cultured synovial cells: a transfection study. J Rheumatol 20: 422-428, 1993.
5. Kuroki Y, Shiozawa S, Sugimoto T, Kanatani M, Kaji H, Miyachi A and Chihara K: Constitutive c-fos expression in osteoblastic MC3T3-E1 cells stimulates osteoclast maturation and osteoclastic bone resorption. Clin Exp Immunol 95: 536-539, 1994.
6. Shiozawa S, Shimizu K, Tanaka K and Hino K: Studies on the contribution of c-fos/AP-1 to arthritic joint destruction. J Clin Invest 99: 1210-1216, 1997.
7. Kawasaki H, Komai K, Ouyang Z, Murata M, Hikasa M, Ohgiri M and Shiozawa S: c-Fos/activator protein-1 transactivates wee1 kinase at G(1)/S to inhibit premature mitosis in antigen-specific Th1 cells. EMBO J 20: 4618-4627, 2001.
8. Piechaczyk M and Blanchard JM: c-fos proto-oncogene regulation and function. Crit Rev Oncol Hematol 17: 93-131, 1994.
9. Mechta-Grigoriou F, Gerald D and Yaniv M: The mammalian Jun proteins: redundancy and specificity. Oncogene 20: 2378-2389, 2001.
10. Wakisaka S, Suzuki N, Saito N, Ochi T and Sakane T: Possible correction of abnormal rheumatoid arthritis synovial cell function by junD transfection *in vitro*. Arthritis Rheum 41: 470-481, 1998.
11. Sickinger S and Kinne RW: Possible correction of abnormal rheumatoid arthritis synovial cell function by junD transfection *in vitro*: comment on the article by Wakisaka *et al*. Arthritis Rheum 43: 945-946, 2000.
12. Winfield JB: Stress proteins, arthritis, and autoimmunity. Arthritis Rheum 32: 1497-1504, 1989.
13. Whitesell L, Mimnaugh EG, De Costa B, Myers CE and Neckers LM: Inhibition of heat shock protein HSP90-pp60v-src heteroprotein complex formation by benzoquinone ansamycins: essential role for stress proteins in oncogenic transformation. Proc Natl Acad Sci USA 91: 8324-8328, 1994.
14. Piper PW: The Hsp90 chaperone as a promising drug target. Curr Opin Investig Drugs 2: 1606-1610, 2001.
15. Shiotsu Y, Neckers LM, Wortman I, An WG, Schulte TW, Soga S, Murakata C, Tamaoki T and Akinaga S: Novel oxime derivatives of radicicol induce erythroid differentiation associated with preferential G(1) phase accumulation against chronic myelogenous leukemia cells through destabilization of Bcr-Abl with Hsp90 complex. Blood 96: 2284-2291, 2000.
16. Carter KD and Panek JS: Total synthesis of herbimycin A. Org Lett 6: 55-57, 2004.
17. Neckers L: Hsp90 inhibitors as novel cancer chemotherapeutic agents. Trends Mol Med 8: S55-S61, 2002.
18. Arnett FC, Edworthy SM, Bloch DA, McShane DJ, Fries JF, Cooper NS, Healey LA, Kaplan SR, Liang MH, Luthra HS, *et al*: The American Rheumatism Association 1987 revised criteria for the classification of rheumatoid arthritis. Arthritis Rheum 31: 315-324, 1988.
19. Arend WP and Dayer JM: Cytokines and cytokine inhibitors or antagonists in rheumatoid arthritis. Arthritis Rheum 33: 305-315, 1990.
20. Feldmann M, Brennan FM and Maini RN: Role of cytokines in rheumatoid arthritis. Annu Rev Immunol 14: 397-440, 1996.
21. Trabandt A, Aicher WK, Gay RE, Sukhatme VP, Fassbender HG and Gay S: Spontaneous expression of immediately-early response genes c-fos and egr-1 in collagenase-producing rheumatoid synovial fibroblasts. Rheumatol Int 12: 53-59, 1992.
22. Asahara H, Fujisawa K, Kobata T, Hasunuma T, Maeda T, Asanuma M, Ogawa N, Inoue H, Sumida T and Nishioka K: Direct evidence of high DNA binding activity of transcription factor AP-1 in rheumatoid arthritis synovium. Arthritis Rheum 40: 912-918, 1997.
23. Shimizu K, Kawasaki H, Morisawa T, Nakamura M, Yamamoto E, Yoshikawa N, Doita M, Shiozawa K, Yonehara S, Chihara K, *et al*: Spontaneous and cytokine regulated c-fos gene expression in rheumatoid synovial cells: resistance to cytokine stimulation when the c-fos gene is overexpressed. Ann Rheum Dis 59: 636-640, 2000.
24. Jain J, Valge-Archer VE and Rao A: Analysis of the AP-1 sites in the IL-2 promoter. J Immunol 148: 1240-1250, 1992.
25. Boise LH, Petryniak B, Mao X, June CH, Wang CY, Lindsten T, Bravo R, Kovary K, Leiden JM and Thompson CB: The NFAT-1 DNA binding complex in activated T cells contains Fra-1 and JunB. Mol Cell Biol 13: 1911-1919, 1993.
26. Benderdour M, Tardif G, Pelletier JP, Di Battista JA, Reboul P, Ranger P and Martel-Pelletier J: Interleukin 17 (IL-17) induces collagenase-3 production in human osteoarthritic chondrocytes via AP-1 dependent activation: differential activation of AP-1 members by IL-17 and IL-1beta. J Rheumatol 29: 1262-1272, 2002.
27. Huber R, Kunisch E, Gluck B, Egerer R, Sickinger S and Kinne RW: Comparison of conventional and real-time RT-PCR for the quantitation of jun protooncogene mRNA and analysis of junB mRNA expression in synovial membranes and isolated synovial fibroblasts from rheumatoid arthritis patients. Z Rheumatol 62: 378-389, 2003.
28. Meixner A, Karreth F, Kenner L and Wagner EF: JunD regulates lymphocyte proliferation and T helper cell cytokine expression. EMBO J 23: 1325-1335, 2004.
29. Szremska AP, Kenner L, Weisz E, Ott RG, Passegue E, Artwohl M, Freissmuth M, Stoxreiter R, Theussl HC, Parzer SB, *et al*: JunB inhibits proliferation and transformation in B-lymphoid cells. Blood 102: 4159-4165, 2003.
30. Hirai SI, Ryseck RP, Mechta F, Bravo R and Yaniv M: Characterization of junD: a new member of the jun proto-oncogene family. EMBO J 8: 1433-1439, 1989.
31. Schaefer LK, Wang S and Schaefer TS: Functional interaction of Jun and homeodomain proteins. J Biol Chem 276: 43074-43082, 2001.
32. Stephanou A, Amin V, Isenberg DA, Akira S, Kishimoto T and Latchman DS: Interleukin 6 activates heat-shock protein 90 beta gene expression. Biochem J 321: 103-106, 1997.
33. Hayem G, De Bandt M, Palazzo E, Roux S, Combe B, Eliaou JF, Sany J, Kahn MF and Meyer O: Anti-heat shock protein 70 kDa and 90 kDa antibodies in serum of patients with rheumatoid arthritis. Ann Rheum Dis 58: 291-296, 1999.
34. Sugita T, Tanaka S, Murakami T, Miyoshi H and Ohnuki T: Immunosuppressive effects of the heat shock protein 90-binding antibiotic geldanamycin. Biochem Mol Biol Int 47: 587-595, 1999.
35. Freeman BC and Yamamoto KR: Disassembly of transcriptional regulatory complexes by molecular chaperones. Science 296: 2232-2235, 2002.
36. Okazaki S, Ito T, Ui M, Watanabe T, Yoshimatsu K and Iba H: Two proteins translated by alternative usage of initiation codons in mRNA encoding a JunD transcriptional regulator. Biochem Biophys Res Commun 250: 347-353, 1998.

Estrogen specifically stimulates expression and production of osteoprotegerin from rheumatoid synovial fibroblasts

MAKOTO MITANI[1], YASUSHI MIURA[1,2], RYUICHI SAURA[1,2], ATSUSHI KITAGAWA[1], TAIHEI FUKUYAMA[1], AKIRA HASHIRAMOTO[2], SHUNICHI SHIOZAWA[2], MASAHIRO KUROSAKA[1] and SHINICHI YOSHIYA[1]

[1]Department of Orthopaedic Surgery, Kobe University, Graduate School of Medicine; [2]Department of Rheumatology, Kobe University, Faculty of Health Sciences School of Medicine, Kobe, Japan

Abstract. We studied the effects of estrogen on human fibroblast-like synovial cells in rheumatoid arthritis (RA-FLS) focusing on receptor activator of NF-κB ligand (RANKL) and its decoy receptor osteoprotegerin (OPG), the osteoclast formation and function regulators that have a substantial role in bone erosion of RA. Estrogen influences osteoporosis and the onset of RA clinically. The cellular responses of RA-FLS to estrogen are initiated via two high-affinity estrogen receptors (ERs). Culture of RA-FLS in the presence of 10^{-6} M 17ß-estradiol (E2) increased expression of estrogen receptor (ER)-α, but not ER-ß. OPG mRNA expression was significantly increased, whereas RANKL mRNA was unaffected. E2 treatment also significantly increased the amount of OPG released in the culture supernatant. The increase of OPG and ER-α was specifically antagonized by the pure estrogen antagonist ICI 182780. Tamoxifen, a selective ER moderator, did not increase OPG. The results indicate that estrogen stimulates secretion of OPG from RA-FLS by acting on ER-α, which likely prevents bone erosion in RA.

Introduction

Periarticular bone erosion is the beginning of devastating rheumatic joint destruction (1,2). Bone-resorbing osteoclasts formed in the synovial tissues have important roles in rheumatoid bone destruction (3-6). Molecules important for osteoclastogenesis, including receptor activator of NF-κB ligand (RANKL) and osteoprotegerin (OPG), are expressed in human fibroblast-like synovial cells of rheumatoid arthritis (RA-FLS) (6,7). RANKL is a membrane-bound molecule that binds to the osteoclast precursors to regulate osteoclast formation (8-10). OPG, a soluble tumor necrosis factor (TNF) receptor-like molecule termed TNF receptor superfamily 11B, is a naturally occurring RANKL inhibitor. OPG competitively binds RANKL to inhibit the action of the receptor activator of NF-κB (RANK) both *in vivo* and *in vitro*, which prevents osteoclastic bone resorption (9-11). Hence, RANKL expressed on synovial fibroblasts induces rheumatoid bone erosion by generating periarticular osteoclasts, and this process is inhibited by endogenous and exogenous OPG (6).

The effect of sex hormones cannot be dismissed in the pathogenesis of RA (12,13), because RA is predominant in premenopausal women, whereas the prevalence of RA is almost equal in older men and women (14,15). The clinical severity and symptoms of RA are under the influence of the hormonal environments, including pregnancy, delivery, and menstrual cycles (14,16,17). Among sex hormones, estrogen is essential for bone metabolism. Estrogens diffuse in and out of cells to bind nuclear estrogen receptor (ER) proteins. The effects of estrogens are mediated by two distinct nuclear receptors, ER-α and ER-ß, encoded by separate genes and located on different chromosomes (18-21). ER-α and ER-ß are expressed in RA-FLS (22), and estrogen inhibits bone resorption by stimulating OPG in osteoblasts and mouse stromal cells (23,24).

We studied the effect of 17ß-estradiol (E2) on the expression of OPG and RANKL in RA-FLS, in relation to the expression of ER-α and ER-ß.

Materials and methods

Cell preparation. Synovial tissues were obtained during joint surgery from patients with RA fulfilling the criteria of the American College of Rheumatology (25) and OA, in accordance with the World Medical Association Declaration of Helsinki Ethical Principles for Medical Research Involving Human Subjects. Tissues were minced and digested in a solution containing 0.2% collagenase (Sigma Chemical Co., St. Louis, MO) and 0.25% trypsin-ethylenediamine tetraacetic acid (trypsin-EDTA; Difco Laboratories, Detroit, MI) at 37°C for 2 h. Dissociated cells were cultured in Dulbecco's modified Eagle's medium (DMEM; Gibco BR, Grand Island, NY) supplemented with 10% fetal bovine serum (FBS; Biowhittaker, Walkersville, ML) and 100 U/ml penicillin-streptomycin in a tissue culture flask (Corning Inc., Corning, NY) at a cell density of 1.0×10^5 cells/cm^2. After overnight

Correspondence to: Dr Yasushi Miura, Department of Orthopaedic Surgery, Kobe University, Graduate School of Medicine, 7-5-1 Kusunoki-cho, Chuo-ku, Kobe 650-0017, Japan
E-mail: miura@kobe-u.ac.jp

Key words: estrogen, estrogen receptor, osteoprotegerin, receptor activator of NF-κB ligand, rheumatoid arthritis, synovial cell

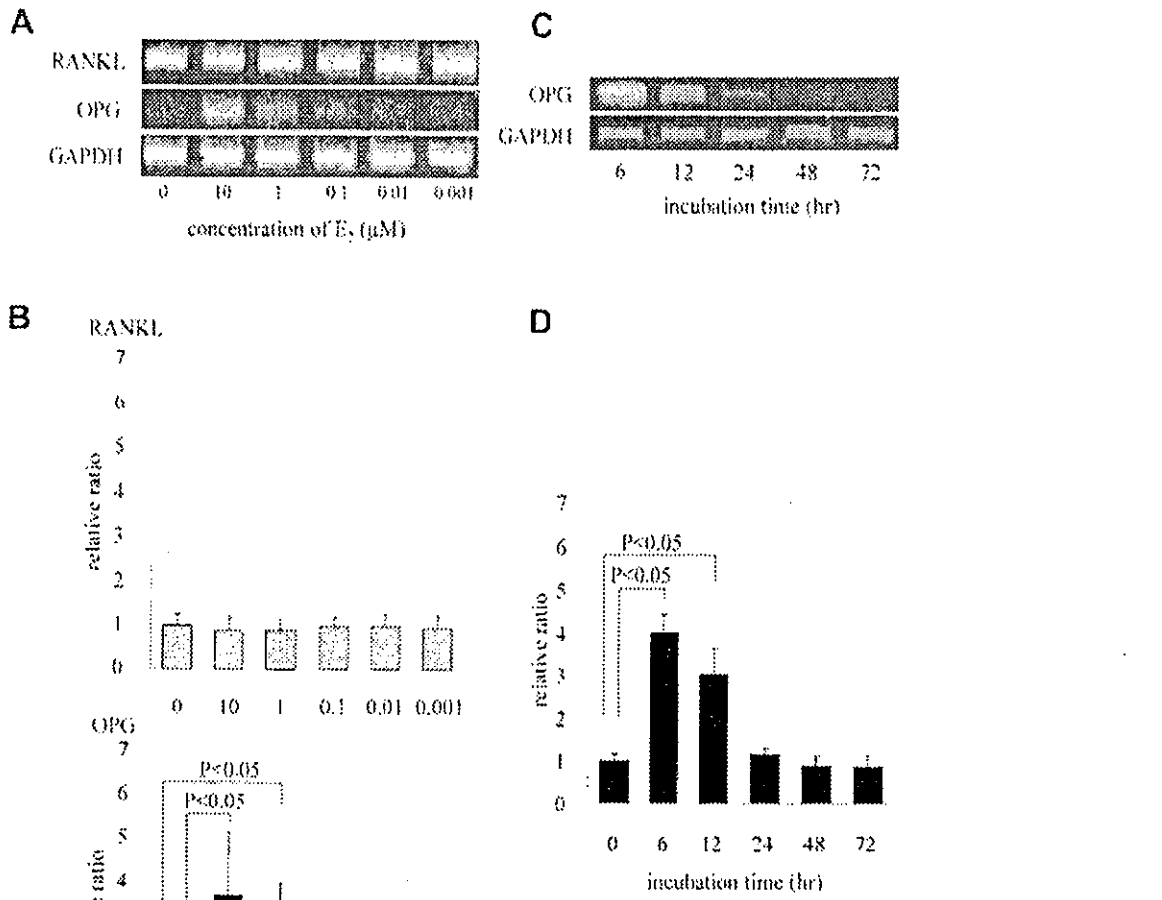

Figure 2. Expression of RANKL and OPG mRNA in RA-FLS treated with E2. (A), Dose dependency: RA-FLS were incubated with various concentrations of E2 (10^{-5}-10^{-9} M) for 12 h or untreated. (B), Fold increases of RANKL (upper panel) and OPG (lower panel) mRNA by E2 treatment. E2 enhanced OPG mRNA expression at the concentrations of 10^{-6} and 10^{-5} M ($P<0.05$), but did not increase RANKL mRNA. (C), Time-course study: RA-FLS were treated with 10^{-6} M E2 for the incubation period indicated. (D), Fold increases of RANKL and OPG mRNA of time-course study. The effect of E2 reached the peak at 6 h, declined thereafter for 12 h and was almost abolished after 24 h ($P<0.05$).

and CATGTGGGCCATGAGGTCCACCAC. After PCR amplification, 8 μl aliquots of the PCR products were electrophoresed in 2.0% agarose gels and stained with ethidium bromide. PCR products were photographed and quantified using the public domain NIH Image program (developed at the US National Institutes of Health and available on the Internet at http://rsb.info.nih.gov/nih-image/). Values were normalized to GAPDH expression.

Enzyme-linked immunosorbent assay OPG assay. RA-FLS were cultured in a 24-well plate at a cell density of 1.0×10^5/well in DMEM supplemented with 10% FBS. When the cultured RA-FLS reached confluence, they were incubated with E2 or tamoxifen. After 6, 12, 24, and 48 h of incubation, the concentration of OPG in the culture supernatants was measured with using OPG enzyme-linked immunosorbent assay system (Immundiagnostik, Bensheim, Germany) according to the manufacturer's instructions. The OPG concentration was determined from the mean value of triplicate samples. Statistical analyses were performed by One-way ANOVA and Fisher's PLSD. A $P<0.05$ were considered to be statistically significant.

Results

Expression of ER-α and ER-β mRNA in RA-FLS. To determine the presence of ER-α and ER-ß in FLS, we utilized RT-PCR to amplify ER mRNA from FLS of patients with RA and osteoarthritis (OA) (Fig. 1A). The results indicated that mRNA of ER-α and ER-ß was specifically amplified in all 6 RA and 5 OA samples, the specificity of which was confirmed by DNA sequencing (data not shown). The effect of E2 on the expression of ER-α and ER-ß was examined in RA-FLS using RT-PCR; E2 significantly enhanced ER-α mRNA expression in RA-FLS in a dose-dependent manner ($P<0.05$), whereas ER-ß mRNA expression was unaffected (Fig. 1B and C). Co-treatment with a specific estrogen antagonist, ICI 182780, completely abrogated the stimulatory effects of E2 (10^{-6} M) on ER-α in RA-FLS (Fig. 1D and E).

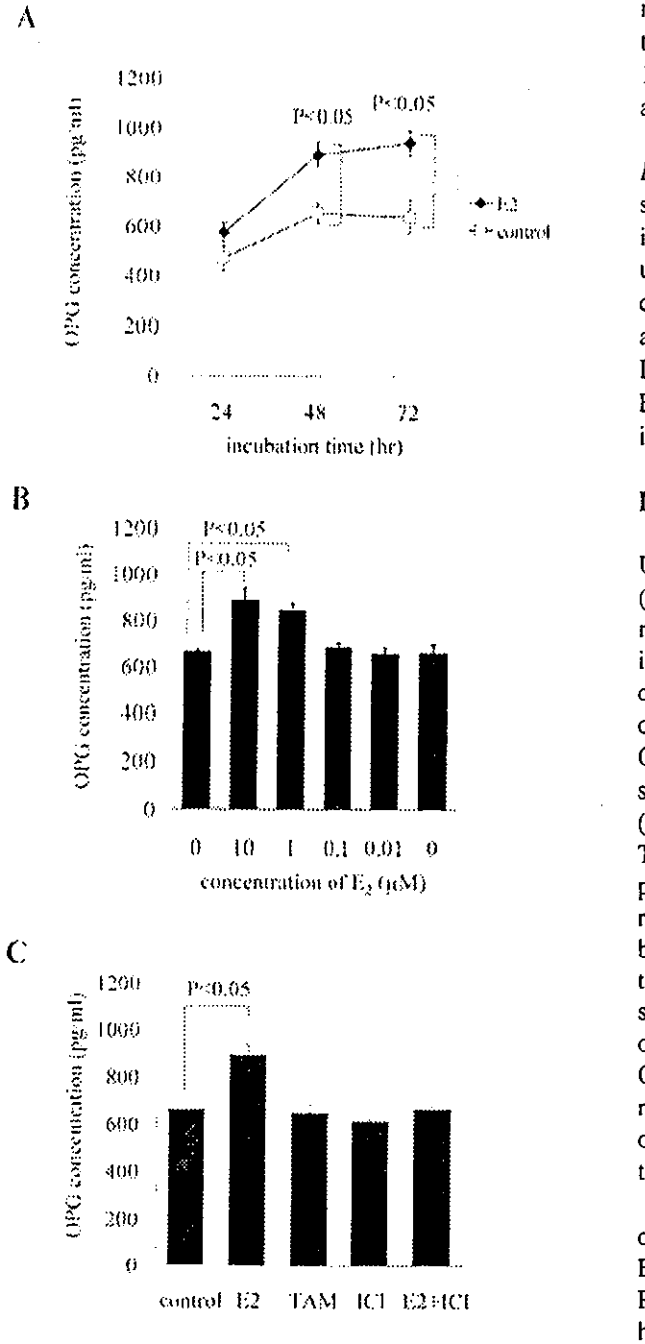

Figure 3. E2-induced OPG protein secretion from RA-FLS. (A), Time dependency: RA-FLS were treated with 10^{-6} M E2 for the incubation period indicated. The values are given as the mean ± SEM of triplicates (P<0.05). OPG secreted by RA-FLS treated with 10^{-6} M E2 was significantly higher than untreated RA-FLS at 48 and 72 h (P<0.05). (B), Dose dependency: RA-FLS were treated with various concentrations of E2 (10^{-5}-10^{-9} M) for 12 h or untreated. Treatment with E2 at the concentrations of 10^{-6} and 10^{-5} M increased OPG secretion from RA-FLS at 48 h (P<0.05). (C), Treatment with tamoxifen (TAM) and ICI 182780 (ICI). Co-treatment with 10^{-5} M ICI 182780 completely abrogated the stimulatory effects of E2 (10^{-6} M) on OPG secretion. Tamoxifen (10^{-6} M) did not increase OPG secretion from RA-FLS.

mRNA expression of OPG and RANKL in RA-FLS. RT-PCR indicated that E2 enhanced OPG mRNA expression at concentrations greater than 10^{-6} M (P<0.05), whereas RANKL mRNA expression was unaffected (Fig. 2A and B). A time-course study revealed that 10^{-6} M of E2 enhanced OPG mRNA expression as early as 6 h after treatment, and that the effect of E2 peaked at 6 h and declined thereafter, up to 12 h (P<0.05; Fig. 2C and D). The effect of E2 was almost abolished after 24 h.

Effect on OPG secretion in RA-FLS. The amount of OPG secreted from RA-FLS to culture supernatants was significantly increased after treatment with 10^{-6} M E2, as compared with untreated controls at 48 and 72 h (P<0.05) (Fig. 3A). E2 at concentrations greater than 10^{-6} M increased OPG secretion after 48 h (P<0.05; Fig. 3B). While co-treatment with 10^{-5} M ICI 182780 completely abrogated the stimulatory effects of E2 (10^{-6} M) on OPG secretion, tamoxifen (10^{-6} M) did not increase OPG secretion from RA-FLS (Fig. 3C).

Discussion

Until recently, inflammatory cytokines, such as interleukin (IL)-1, IL-6, IL-11, and TNF-α, were implicated as important mediators of bone lysis (26-28). Recent findings, however, indicate that osteoclasts have a substantial role in bone destruction, and that RANKL might be the central mediator of osteoclast development in RA and other bone loss pathologies. Osteoclasts are observed at the invasive front of granulomatous synovial tissues in both RA and animal models of arthritis (5,29). RANKL expressed on synovial fibroblasts and activated T lymphocytes enhances differentiation of synovial macrophages and osteoclast precursors in bone marrow into bone-resorbing osteoclasts, and activates osteoclasts at sites of bone erosion in RA (6,30,31). Further, Kong *et al* reported that joint destruction, but not synovial inflammation, was significantly improved by OPG treatment in rodent models of adjuvant arthritis (32). While RANK, RANKL, and OPG are all expressed in rheumatoid synovial tissues, their relative balance is important for determining the extent of osteoclastic bone resorption and is considered to be a good therapeutic target (6,7,28).

We demonstrate that 17ß-estradiol enhances the expression of ER-α in RA-FLS without affecting the expression of ER-ß and that E2 stimulates the production of OPG from RA-FLS without affecting RANKL expression. We therefore hypothesize that estrogen prevents bone erosion by up-regulating OPG production from RA-FLS via ER-α to increase OPG binding of RANKL, which subsequently blocks the interaction between RANKL and RANK in osteoclasts.

Despite the number of studies performed to date, the effect of sex hormones on RA remains controversial. *In vitro* studies indicate that estrogen regulates proteinases and inflammatory cytokines, such as matrix metalloproteinase (MMP) and IL-1ß-induced IL-6, and thus estrogen potentiates the destruction of cartilage and bone in RA (12,13). Positive and negative results have been reported with regard to hormone replacement therapy (HRT) with estrogens (33-37). Nevertheless, type-II collagen-induced arthritis in female mice is exacerbated by ovariectomy and is ameliorated by subsequent treatment with E2 (38). Furthermore, a recent trial exploring the effects in RA demonstrated that HRT significantly ameliorated inflammation, disease activity, and osteoporosis of RA, and retarded the progression of joint destruction (39).

In the present study we demonstrated that 17ß-estradiol increases ER-α mRNA and OPG mRNA expression, and the OPG protein released in the culture supernatant was simultaneously increased in each line of RA-FLS. Importantly, the increase of OPG and ER-α was specifically antagonized by ICI 182780, an estrogen specific antagonist. Further, in RA-FLS, OPG, but not RANKL, was increased by 17ß-estradiol.

Interestingly, a selective ER modulator (SERM), tamoxifen, which acts as a weak estrogen agonist on bone *in vivo*, did not affect OPG production of RA-FLS. As tamoxifen is reported to abrogate the effect of E2 to increase MMP in RA-FLS (12), tamoxifen might function as an antagonist rather than as an agonist of E2 in RA-FLS. Raloxifene, a SERM member, however, stimulates OPG and inhibits IL-6 production in human trabecular osteoblasts (40). Further studies regarding the modulation of OPG production of RA-FLS, SERMs, and the other modulators will be important to prevent bone erosion on RA.

References

1. Shimizu S, Shiozawa S, Shiozawa K, Imura S and Fujita T: Quantitative histologic studies on the pathogenesis of periarticular osteoporosis in rheumatoid arthritis. Arthritis Rheum 28: 25-31, 1985.
2. Van Zeben D, Hazes JM, Breedveld FC, Zwinderman AH and Vandenbroucke JP: Which clinical variables contribute to the physician's assessment of medium term outcome in rheumatoid arthritis? J Rheumatol 20: 33-39, 1993.
3. Fujikawa Y, Shingu M, Torisu T, Itonaga I and Masumi S: Bone resorption by tartrate-resistant acid phosphatase-positive multinuclear cells isolated from rheumatoid synovium. Br J Rheumatol 35: 213-217, 1996.
4. Takayanagi H, Oda H, Yamamoto S, Kawaguchi H, Tanaka S, Nishikawa T and Koshihara Y: A new mechanism of bone destruction in rheumatoid arthritis: synovial fibroblasts induce osteoclastogenesis. Biochem Biophys Res Commun 240: 279-286, 1997.
5. Gravallese EM, Harada Y, Wang JT, Gorn AH, Thornhill TS and Goldring SR: Identification of cell types responsible for bone resorption in rheumatoid arthritis and juvenile rheumatoid arthritis. Am J Pathol 152: 943-951, 1998.
6. Takayanagi H, Iizuka H, Juji T, Nakagawa T, Yamamoto A, Miyazaki T, Koshihara Y, Oda H, Nakamura K and Tanaka S: Involvement of receptor activator of nuclear factor kappaB ligand/osteoclast differentiation factor in osteoclastogenesis from synoviocytes in rheumatoid arthritis. Arthritis Rheum 43: 259-269, 2000.
7. Haynes DR, Crotti TN, Loric M, Bain GI, Atkins GJ and Findlay DM: Osteoprotegerin and receptor activator of nuclear factor kappaB ligand (RANKL) regulate osteoclast formation by cells in the human rheumatoid arthritic joint. Rheumatology 40: 623-630, 2001.
8. Yasuda H, Shima N, Nakagawa N, Yamaguchi K, Kinosaki M, Mochizuki S, Tomoyasu A, Yano K, Goto M, Murakami A, Tsuda E, Morinaga T, Higashio K, Udagawa N, Takahashi N and Suda T: Osteoclast differentiation factor is a ligand for osteoprotegerin/osteoclastogenesis-inhibitory factor and is identical to TRANCE/RANKL. Proc Natl Acad Sci USA 95: 3597-3602, 1998.
9. Lacey DL, Timms E, Tan HL, Kelley MJ, Dunstan CR, Burgess T, Elliott R, Colombero A, Elliott G, Scully S, Hsu H, Sullivan J, Hawkins N, Davy E, Capparelli C, Eli A, Qian YX, Kaufman S, Sarosi I, Shalhoub V, Senaldi G, Guo J, Delaney J and Boyle WJ: Osteoprotegerin ligand is a cytokine that regulates osteoclast differentiation and activation. Cell 93: 165-176, 1998.
10. Simonet WS, Lacey DL, Dunstan CR, Kelley M, Chang MS, Luthy R, Nguyen HQ, Wooden S, Bennett L, Boone T, Shimamoto G, De Rose M, Elliott R, Colombero A, Tan HL, Trail G, Sullivan J, Davy E, Bucay N, Renshaw-Gegg L, Hughes TM, Hill D, Pattison W, Campbell P, Boyle WJ, *et al*: Osteoprotegerin: a novel secreted protein involved in the regulation of bone density. Cell 89: 309-319, 1997.
11. Yasuda H, Shima N, Nakagawa N, Mochizuki SI, Yano K, Fujise N, Sato Y, Goto M, Yamaguchi K, Kuriyama M, Kanno T, Murakami A, Tsuda E, Morinaga T and Higashio K: Identity of osteoclastogenesis inhibitory factor (OCIF) and osteo-protegerin (OPG): a mechanism by which OPG/OCIF inhibits osteoclastogenesis *in vitro*. Endocrinology 139: 1329-1337, 1998.
12. Khalkhali-Ellis Z, Seftor EA, Nieva DR, Handa RJ, Price RH, Jr, Kirschmann DA, Baragi VM, Sharma RV, Bhalla RC, Moore TL and Hendrix MJ: Estrogen and progesterone regulation of human fibroblast-like synoviocyte function *in vitro*: implications in rheumatoid arthritis. J Rheumatol 27: 1622-1631, 2000.
13. Kawasaki T, Ushiyama T, Inoue K and Hukuda S: Effects of estrogen on interleukin-6 production in rheumatoid fibroblast-like synoviocytes. Clin Exp Rheumatol 18: 743-745, 2000.
14. Masi AT: Hormonal and immunologic risk factors for the development of rheumatoid arthritis: an integrative physiopathogenetic perspective. Rheum Dis Clin North Am 26: 775-803, 2000.
15. Masi AT: Incidence of rheumatoid arthritis: do the observed age-sex interaction patterns support a role of androgenic-anabolic steroid deficiency in its pathogenesis? Br J Rheumatol 33: 697-699, 1994.
16. Rudge SR, Kowanko IC and Drury PL: Menstrual cyclicity of finger joint size and grip strength in patients with rheumatoid arthritis. Ann Rheum Dis 42: 425-430, 1983.
17. Persellin RH: The effect of pregnancy on rheumatoid arthritis. Bull Rheum Dis 27: 922-927, 1976.
18. Katzenellenbogen BS: Estrogen receptors: bioactivities and interactions with cell signaling pathways. Biol Reprod 54: 287-293, 1996.
19. Kuiper GG, Enmark E, Pelto-Huikko M, Nilsson S and Gustafsson JA: Cloning of a novel receptor expressed in rat prostate and ovary. Proc Natl Acad Sci USA 93: 5925-5930, 1996.
20. Greene GL, Gilna P, Waterfield M, Baker A, Hort Y and Shine J: Sequence and expression of human estrogen receptor complementary DNA. Science 231: 1150-1154, 1986.
21. Tora L, White J, Brou C, Tasset D, Webster N, Scheer E and Chambon P: The human estrogen receptor has two independent nonacidic transcriptional activation functions. Cell 59: 477-487, 1989.
22. Ishizuka M, Hatori M, Suzuki T, Miki Y, Damel AD, Tazawa C, Sawai T, Uzuki M, Tanaka Y, Kokubun S and Sasano H: Sex steroid receptors in rheumatoid arthritis. Clin Sci 00: 000-000, 2003.
23. Bord S, Ireland DC, Beavan SR and Compston JE: The effects of estrogen on osteoprotegerin, RANKL, and estrogen receptor expression in human osteoblasts. Bone 32: 136-141, 2003.
24. Hofbauer LC, Khosla S, Dunstan CR, Lacey DL, Spelsberg TC and Riggs BL: Estrogen stimulates gene expression and protein production of osteoprotegerin in human osteoblastic cells. Endocrinology 140: 4367-4370, 1999.
25. Arnett FC, Edworthy SM, Bloch DA, McShane DJ, Fries JF, Cooper NS, Healey LA, Kaplan SR, Liang MH, Luthra HS, *et al*: The American Rheumatism Association 1987 revised criteria for the classification of rheumatoid arthritis. Arthritis Rheum 31: 315-324, 1988.
26. Chu CQ, Field M, Allard S, Abney E, Feldmann M and Maini RN: Detection of cytokines at the cartilage/pannus junction in patients with rheumatoid arthritis: implications for the role of cytokines in cartilage destruction and repair. Br J Rheumatol 31: 653-661, 1992.
27. Deleuran BW, Chu CQ, Field M, Brennan FM, Katsikis P, Feldmann M and Maini RN: Localization of interleukin-1 alpha, type 1 interleukin-1 receptor and interleukin-1 receptor antagonist in the synovial membrane and cartilage/pannus junction in rheumatoid arthritis. Br J Rheumatol 31: 801-809, 1992.
28. Kotake S, Udagawa N, Hakoda M, Mogi M, Yano K, Tsuda E, Takahashi K, Furuya T, Ishiyama S, Kim KJ, Saito S, Nishikawa T, Takahashi N, Togari A, Tomatsu T, Suda T and Kamatani N: Activated human T cells directly induce osteoclastogenesis from human monocytes: possible role of T cells in bone destruction in rheumatoid arthritis patients. Arthritis Rheum 44: 1003-1012, 2001.
29. Suzuki Y, Nishikaku F, Nakatuka M and Koga Y: Osteoclast-like cells in murine collagen induced arthritis. J Rheumatol 25: 1154-1160, 1998.
30. Gravallese EM, Manning C, Tsay A, Naito A, Pan C, Amento E and Goldring SR: Synovial tissue in rheumatoid arthritis is a source of osteoclast differentiation factor. Arthritis Rheum 43: 250-258, 2000.

31. Schett G, Redlich K and Smolen JS: The role of osteoprotegerin in arthritis. Arthritis Res Ther 5: 239-245, 2003.
32. Kong YY, Feige U, Sarosi I, Bolon B, Tafuri A, Morony S, Capparelli C, Li J, Elliott R, McCabe S, Wong T, Campagnuolo G, Moran E, Bogoch ER, Van G, Nguyen LT, Ohashi PS, Lacey DL, Fish E, Boyle WJ and Penninger JM: Activated T cells regulate bone loss and joint destruction-in adjuvant arthritis through osteoprotegerin ligand. Nature 402: 304-309, 1999.
33. D'Elia HF, Mattsson LA, Ohlsson C, Nordborg E and Carlsten H: Hormone replacement therapy in rheumatoid arthritis is associated with lower serum levels of soluble IL-6 receptor and higher insulin-like growth factor 1. Arthritis Res Ther 5: R202-R209, 2003.
34. Brennan P, Bankhead C, Silman A and Symmons D: Oral contraceptives and rheumatoid arthritis: results from a primary care-based incident case-control study. Semin Arthritis Rheum 26: 817-823, 1997.
35. Ostensen M: Sex hormones and pregnancy in rheumatoid arthritis and systemic lupus erythematosus. Ann NY Acad Sci 876: 131-144, 1999.
36. Hall GM, Daniels M, Huskisson EC and Spector TD: A randomised controlled trial of the effect of hormone replacement therapy on disease activity in postmenopausal rheumatoid arthritis. Ann Rheum Dis 53: 112-116, 1994.
37. Van den Brink HR, van Everdingen AA, van Wijk MJ, Jacobs JW and Bijlsma JW: Adjuvant oestrogen therapy does not improve disease activity in postmenopausal patients with rheumatoid arthritis. Ann Rheum Dis 52: 862-865, 1993.
38. Holmdahl R, Jansson L, Meyerson B and Klareskog L: Oestrogen induced suppression of collagen arthritis: I. Long term oestradiol treatment of DBA/1 mice reduces severity and incidence of arthritis and decreases the anti type II collagen immune response. Clin Exp Immunol 70: 372-378, 1987.
39. D'Elia HF, Larsen A, Mattsson LA, Waltbrand E, Kvist G, Mellstrom D, Saxne T, Ohlsson C, Nordborg E and Carlsten H: Influence of hormone replacement therapy on disease progression and bone mineral density in rheumatoid arthritis. J Rheumatol 30: 1456-1463, 2003.
40. Viereck V, Grundker C, Blaschke S, Niederkleine B, Siggelkow H, Frosch KH, Raddatz D, Emons G and Hofbauer LC: Raloxifene concurrently stimulates osteoprotegerin and inhibits interleukin-6 production by human trabecular osteoblasts. J Clin Endocrinol Metab 88: 4206-4213, 2003.